CFD ANALYSIS ON SYMMETRIC AND ASYMMETRIC AEROFOIL

A project report submitted in partial fulfilment of the

requirements for the Award of the Degree of

BACHELOR OF ENGINEERING

IN

MECHANICAL ENGINEERING

BY

Pooja Panda	314126520127
K.Lokanath	314126520087
P.Gnana Sai	314126520119
K.Praveen	314126520075
M.Kiran	314126520103

Under the guidance of

Mrs. K.Sree Sruthi (*M.Tech)*

Assistant Professor

DEPARTMENT OF MECHANICAL ENGINEERING

ANIL NEERUKONDA INSTITUTE OF TECHNOLOGY AND SCIENCES

(Affiliated to Andhra University, Accredited by NBA & NAAC)

SANGIVALASA-531162

2014-2018

ANIL NEERUKONDA INSTITUTE OF TECHNOLOGY & SCIENCES

(Affiliated to Andhra University, Approved by AICTE, Accredited by NBA & NAAC with A grade)
SANGIVALASA, VISAKHAPATNAM (District) – 531162

PRAGNANAM BRAHMA
ANITS

CERTIFICATE

This is to certify that the Project Report entitled "**CFD ANALYSIS ON SYMENTRIC AND ASYMETRIC AEROFOIL**" being submitted by POOJA PANDA (314126520127), KOTTAPU LOKANATH (314126520087), PEDAGOPU GNANA SAI (314126520119), KANITI PRAVEEN (314126520075), MUNGARA KIRAN (314126520103) in partial fulfillments for the award of degree of **BACHELOR OF TECHNOLOGY** in **MECHANICAL ENGINEERING** of **ANDHRA UNIVERSITY**. It is the work of bona-fide, carried out under the guidance and supervision of **Mrs. K. Sree Sruthi**, Assistant Professor, Department Of Mechanical Engineering, ANITS during the academic year of 2014-2018.

PROJECT GUIDE

K. Sree Sruthi

(Mrs. K. Sree Sruthi)
Assistant Professor
Mechanical Engineering Department
ANITS, Visakhapatnam.

Approved By

HEAD OF THE DEPARTMENT

(Dr. B. Naga Raju)
Head of the Department
Mechanical Engineering Department
ANITS, Visakhapatnam.

PROFESSOR & HEAD
Department of Mechanical Engineering
ANIL NEERUKONDA INSTITUTE OF TECHNOLOGY & SCIENCES
Sangivalasa-531 162 VISAKHAPATNAM Dist. A.P.

THIS PROJECT IS APPROVED BY THE BOARD OF EXAMINERS

INTERNAL EXAMINER:

Dr. B. Naga Raju
M.Tech,M.E.,Ph.d
Professor & HOD
Dept of Mechanical Engineering
ANITS, Sangivalasa,
Visakhapatnam-531 162.

EXTERNAL EXAMINER:

ACKNOWLEDGEMENT

We express immensely our deep sense of gratitude to Mrs. K Sree Sruthi Assistant Professor, Department of Mechanical Engineering, Anil Neerukonda Institute of Technology & Sciences, Sangivalasa, Bheemunipatnam, Mandal, Visakhapatnam district for her valuable guidance and encouragement at every stage of the work made it a successful fulfilment.

We were very thankful to Prof. T V Hanumantha Rao Principal and Prof. B Naga Raju Head of the Department, Mechanical Engineering Department, Anil Neerukonda Institute of Technology and Sciences, for their valuable suggestions.

We would like to convey our gratitude to each and everyone who have contributed either directly or indirectly and co-operated with us for the successful completion of our work.

Pooja Panda 314126520127

K.Lokanath 314126520087

P.Gnana Sai 314126520119

K.Praveen 314126520075

M.Kiran 314126520103

ABSTRACT

An "aerofoil" is the term used to describe the cross-sectional shape of an object that, when moved through a fluid such as air, creates an aerodynamic force. Aerofoil plays a vital role in any airplane structure whether it is a commercial plane or jet plane. It decides whether the lift force is sufficient to balance the weight or not, the amount of drag force required to be applied on the plane and how these forces are directly related to change in momentum. Aerofoil is basically divided into two categories i.e. Symmetrical and Asymmetrical aerofoil. We have tried to differentiate between the two types i.e. on the basis of their moment, lift, drag coefficients varying with angle of attack, Mach number and magnitude of the coefficients respectively. An attempt has been made to make a detailed study on lift, drag and momentum of various aerofoil's i.e., NACA 0015 and NACA 6409 using CFD tool which is popularly used in this area. The study resulted in deciding the better performing aerofoil is NACA 6409 which is asymmetrical in nature.

LIST OF CONTENTS

LIST OF FIGURES

S.NO **PAGE NO**

LIST OF TABLES

S.NO **PAGE NO**

CHAPTER 1

INTRODUCTION

1.1 AERODYNAMICS

Aerodynamics is an extension of science which is concerned with concentrating on the movement of air, especially when associating with a solid object, such as an aerofoil. Aerodynamics is a sub-field of fluid progress and gas motion, and numerous parts of aerodynamics hypothesis are regular to these fields. The contrast being that "gas dynamics" applies to the investigation of the movement of all gasses, not constrained to air. Formal aerodynamics think about in the cutting edge sense started in the eighteenth century, despite the fact that perceptions of central ideas, for example, aerodynamic drag have been recorded much prior. The vast majority of the early exertions in aerodynamics worked towards attaining heavier-than-air flight, which was initially exhibited by Wilbur and Orville Wright in 1903. From that point forward, the utilization of aerodynamics through scientific examination, observational estimates, wind tunnel experimentation, and workstation recreations has framed the investigative premise for progressing improvements in heavier-than-air flight and various different advances. Work in aerodynamics has concentrated on issues identified with compressible stream, turbulence, and limit layers, and has gotten to be progressively computational in nature.

1.2 STANDARD ATMOSPHERE

The atmospheric layer in which most flying is done is an ever-changing environment. Temperature and pressure vary with altitude, season, location, time, and even sunspot activity. It is impractical to take all of these into consideration when discussing airplane performance. In order to disregard these atmospheric changes, an engineering baseline has been developed called the standard atmosphere**.** It is a set of reference conditions giving representative values of air properties as a function of altitude. Although it is rare to encounter weather conditions that match the standard atmosphere, it is nonetheless representative of average zero humidity conditions at middle latitudes.

The International Organisation for Standardization (ISO) publishes standard atmosphere as international standard, ISO 2533:1975. Other organisations such as

International Civil Aviation Organisation and the United States Government publish extensions or sunsets of the same atmospheric model under heir own standards-making authority.

1.3 FORCES ACTING ON FLIGHT

The four forces of flight are lift, weight, thrust and drag. These forces make an object move up and down, and faster or slower. The amount of each force compared to its opposing force determines how an object moves through the air.

WEIGHT: Gravity is a force that pulls everything down to Earth. Weight is the amount of gravity multiplied by the mass of an object. Weight is also the downward force that an aircraft must overcome to fly. A kite has less mass and therefore less weight to overcome than a jumbo jet, but they both need the same thing in order to fly - lift.

LIFT is the push that lets something move up. It is the force that is the opposite of weight. Everything that flies must have lift. For an aircraft to move upward, it must have more lift than weight. A hot air balloon has lift because the hot air inside is lighter than the air around it. Hot air rises and carries the balloon with it. A helicopter's lift comes from the rotor blades. Their motion through the air moves the helicopter upward. Lift for an airplane comes from its wings.

The shape of an airplane's wings is what makes it possible for the airplane to fly. Airplanes' wings are curved on top and flatter on the bottom. That shape makes airflow over the top faster than under the bottom. As a result, less air pressure is on top of the wing. This lower pressure makes the wing, and the airplane it's attached to, move up. Using curves to affect air pressure is a trick used on many aircraft. Helicopter rotor blades use this curved shape. Lift for kites also come from a curved shape. Even sailboats use this curved shape. A boat's sail is like a wing. That's what makes the sailboat move.

DRAG is a force that pulls back on something trying to move. Drag provides resistance, making it hard to move. For example, it is more difficult to walk or run through water than through air. Water causes more drag than air. The shape of an object also affects the amount of drag. Round surfaces usually have less drag than flat ones. Narrow surfaces usually have less drag than wide ones. The more air that hits a surface, the more the drag the air produces.

THRUST is the force that is the opposite of drag. It is the push that moves something forward. For an aircraft to keep moving forward, it must have more thrust than drag. A small airplane might get its thrust from a propeller. A larger airplane might get its thrust from jet engines. A glider does not have thrust. It can only fly until the drag causes it to slow down and land.

1.4 FLOW CLASSIFICATION

Flow velocity is used to classify flows according to speed regime. Subsonic flows are flow fields in which air velocity throughout the entire flow is below the local speed of sound. Transonic flows include both regions of subsonic flow and regions in which the flow speed is greater than the speed of sound. Supersonic flows are defined to be flows in which the flow speed is greater than the speed of sound everywhere. A fourth classification, hypersonic flow, refers to flows where the flow speed is much greater than the speed of sound. Aerodynamicists disagree on the precise definition of hypersonic flow.

1.4.1 Incompressible Aerodynamics

An incompressible flow is a flow in which density is constant in both time and space. Although all real fluids are compressible, a flow problem is often considered incompressible if the effect of the density changes in the problem on the outputs of interest is small.

Subsonic Flow

Subsonic (or low-speed) aerodynamics studies fluid motion in flows which are much lower than the speed of sound everywhere in the flow.

1.4.2 Compressible Aerodynamics

According to the theory of aerodynamics, a flow is considered to be compressible if its change in density with respect to pressure is non-zero along a streamline. This means that - unlike incompressible flow - changes in density must be considered.

Transonic Flow

The term Transonic refers to a range of flow velocities just below and above the local speed of sound (generally taken as Mach 0.8–1.2). It is defined as the range of speeds between the critical Mach number, when some parts of the airflow over an aircraft become supersonic, and a higher speed, typically near Mach 1.2, when all of

the airflow is supersonic. Between these speeds, some of the airflow is supersonic, and some is not.

Supersonic Flow

Supersonic aerodynamic problems are those involving flow speeds greater than the speed of sound. Calculating the lift on the Concorde during cruise can be an example of a supersonic aerodynamic problem. Supersonic flow behaves very differently from subsonic flow. The fluid finally does strike the object, it is forced to change its properties -- temperature, density, pressure, and Mach number in an extremely violent and irreversible fashion called a shock wave. The presence of shock waves, along with the compressibility effects of high-flow velocity fluids, is the central difference between supersonic and subsonic aerodynamics problems.

Hypersonic Flow

In aerodynamics, hypersonic speeds are speeds that are highly supersonic. In the 1970s, the term generally came to refer to speeds of Mach 5 (5 times the speed of sound) and above. The hypersonic regime is a subset of the supersonic regime. Hypersonic flow is characterized by high temperature flow behind a shock wave, viscous interaction, and chemical dissociation of gas.

1.5 BOUNDARY LAYER

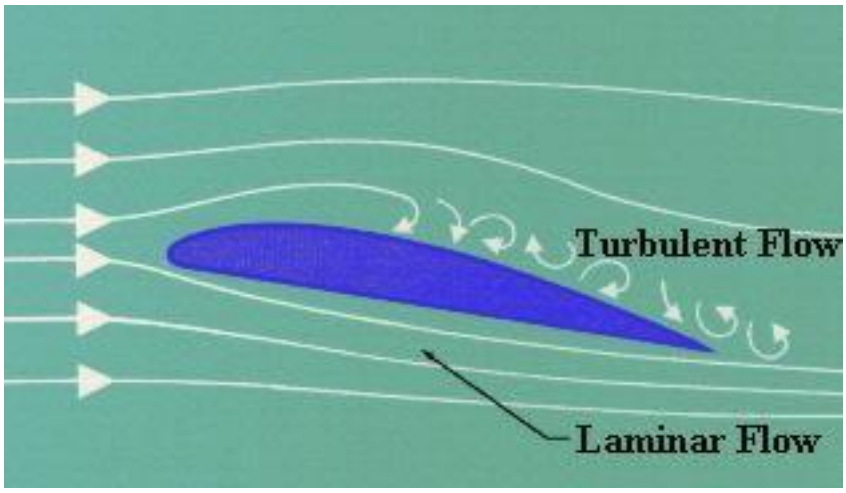

Fig1.1 Boundary Layer

The boundary layer is a very thin layer of air flowing over the surface of an aircraft wing, or aerofoil, (as well as other surfaces of the aircraft).The molecules directly touching the surface of the wing are virtually motionless. Each layer of molecules

hitting the boundary layer moves faster than the layer that is close to the surface of the wing. At the top of the boundary layer, the molecules move at the same speed as the molecules outside the boundary layer. This speed is called the free-stream velocity. The actual speeds at which the molecule move depends upon the shape of the wing, the viscosity, or stickiness, of the air, and its compressibility (how much it can be compacted).

Further boundary layers may be either laminar (layered), or turbulent (disordered). As the boundary layer moves toward the centre of the wing, it begins to lose speed due to skin friction drag. At its transition point, the boundary layer changes from laminar, where the velocity changes uniformly as one moves away from the object surface, to turbulent, where the velocity is characterized by unsteady (changing with time) swirling flows inside the boundary layer.

1.6 AEROFOIL NOMENCLATURE

An airfoil (in American English) or aerofoil (in British English) is the state of a wing or edge or cruise as seen in cross-area. An aerofoil-formed body travelled through a fluid handles an aerodynamic energy. The segment of this power perpendicular to the course of movement is called lift. The segment parallel to the bearing of movement is called drag. Subsonic flight aerofoils have a trademark shape with an adjusted heading edge, emulated by a sharp trailing edge, regularly with uneven camber. Foils of comparative capacity composed with water as the working fluid are called hydrofoils.

The lift on an aerofoil is fundamentally the consequence of its approach and shape. At the point when arranged at a suitable edge, the aerofoil diverts the approaching air, bringing about energy on the aerofoil in the heading inverse to the diversion. This power is known as aerodynamic drive and could be determined into two parts: Lift and drag. Most thwart shapes oblige a positive approach to produce lift; however cambered aerofoils can create lift at zero approach. This "turning" of the air in the region of the aerofoil makes bended streamlines which brings about more level weight on one side and higher weight on the other. This weight contrast is joined by a speed distinction, through Bernoulli's standard, so the ensuing stream field about the aerofoil has a higher normal speed on the upper surface than on the more level surface. The lift power might be connected specifically to the normal top/base speed contrast without registering the weight by utilizing the idea of flow and the Kutta-Joukowski hypothesis.

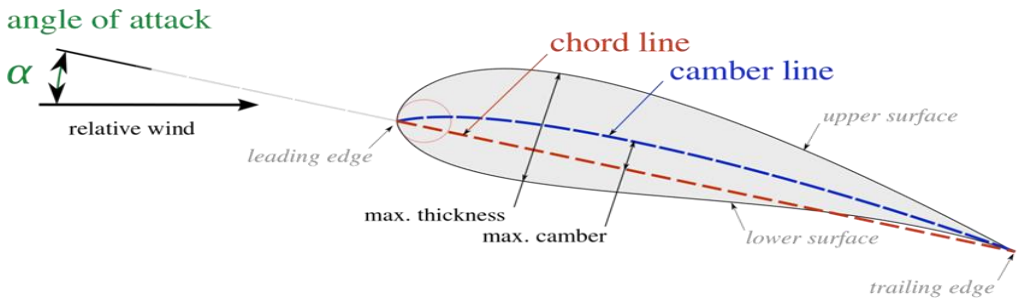

Fig1.2 Aerofoil Nomenclature

- **Leading Edge**: - It is the edge of the aerofoil facing the direction of motion of plane. It is generally roundish in shape and deflects the air in such a way that the velocity of air on upper surface of the aerofoil is more than velocity on the lower surface.
- **Trailing Edge**: - It is the edge of the aerofoil which is pointed in nature. It is located at the back side of the aerofoil.
- C**hord Line**: - Chord Line of an aerofoil is an infinitely long, straight line which passes through its leading and trailing edges. Chord is a measure of the width of an aerofoil. It is measured along the chord line and is the distance from the leading edge to the trailing edge. Chord will typically vary from the wingtip to the wing root. The root chord is the chord at the wing centreline and the tip chord is measured at the wingtip. The average chord (c) is the average of every chord from the wing root to the wingtip.
- **Angle Of Attack**: - It is the angle which the chord line makes with the direction of motion of plane. It is an important parameter which affects the coefficient of lift and drag.
- **Chamber Line**: - It is a line joining leading edge and trailing edge and dividing the aerofoil into two symmetrical parts. It may or may not be a straight line.
- **Lift Coefficient**: - It is a dimensionless coefficient that relates the lifting force on the body to its velocity, surface area and the density of the fluid in which it is lifting.
- **Drag Coefficient**: - It is a dimensionless coefficient that relates the drag force on the body to its velocity, surface area and the density of the fluid in which it is moving.
- **Stall angle of attack**: - It is the angle of attack at which the lift coefficient is maximum and after which the lift coefficient starts to decrease.
- **Wing Area (S)**: - It is the apparent surface area of a wing from wingtip to wingtip. More precisely, it is the area within the outline of a wing in the plane

of its chord, including that area within the fuselage, hull or nacelles. The formula for S is

S=b*c

- **Taper**: - It is the reduction in the chord of an aerofoil from root to tip. The wings of the aircraft are tapered to reduce weight, improve structural stiffness, and reduce wingtip vortices.
  The wing to have straight leading and trailing edges, taper ratio (λ) is the ratio of the tip chord to the root chord.

$$\lambda = \frac{c_T}{c_R}$$

- **Sweep Angle (Λ)**: - It is the angle between the lateral axis and a line drawn 25% aft of the leading edge.

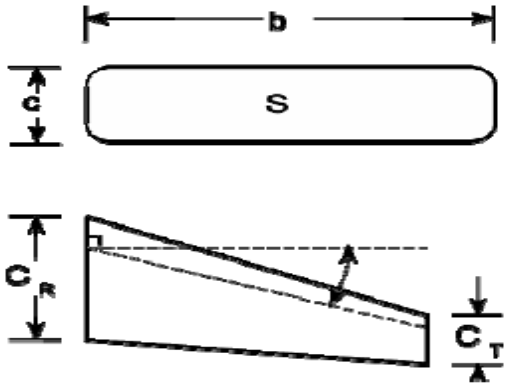

Fig1.3 Sweep Angle

- **Aspect Ratio (AR)**: - It is the ratio of the wingspan to the average chord. An aircraft with a high aspect ratio (35:1), such as a glider, would have a long, slender wing. A low aspect ratio (3:1) indicates a short, stubby wing, such as on a high performance jet.

AR=b/c

- **Wing Loading (WL)**: - It is the ratio of an airplane's weight to the surface area of its wings. There tends to be an inverse relationship between aspect ratio and wing loading. Gliders have high aspect ratios and low wing loading. Fighters with low aspect ratios manoeuvre at high g-loads and are designed with high wing

WL=W/S

- **Angle of incidence**: - The angle of incidence of a wing is the angle between the airplane's longitudinal axis and the chord line of the wing.

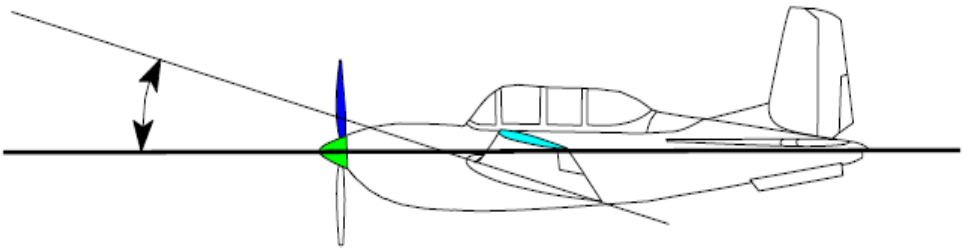

Fig1.4 Angle Of Incidence

- **Dihedral angle**: - It is the angle between the span wise inclination of the wing and the lateral axis. A negative dihedral angle is called an Anhedral angle.

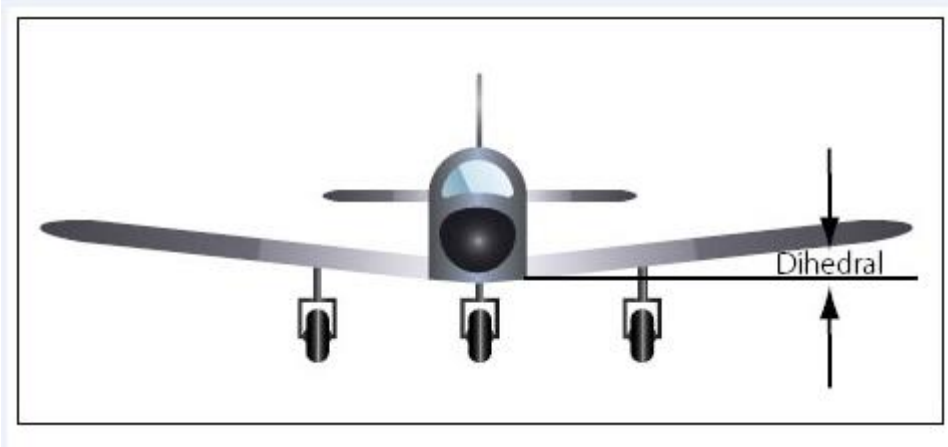

Fig1.5 Dihedral Angle

1.7 NACA AEROFOIL

The early NACA aerofoil series, the 4-digit, 5-digit, and modified 4-/5-digit, were generated using analytical equations that describe the camber (curvature) of the mean-line (geometric centreline) of the aerofoil section as well as the section's thickness distribution along the length of the aerofoil. Later families, including the 6-Series, are more complicated shapes derived using theoretical rather than geometrical methods. Before the National Advisory Committee for Aeronautics (NACA) developed these series, aerofoil design was rather arbitrary with nothing to guide the designer except past experience with known shapes and experimentation with modifications to those shapes.

This methodology began to change in the early 1930s with the publishing of a NACA report entitled "The Characteristics of 78 Related Aerofoil Sections from Tests in the Variable Density Wind Tunnel". In this landmark report, the authors noted that there

were many similarities between the aerofoils that were most successful, and the two primary variables that affect those shapes are the slope of the aerofoil means camber line and the thickness distribution above and below this line. They then presented a series of equations incorporating these two variables that could be used to generate an entire family of related aerofoil shapes. As aerofoil design became more sophisticated, this basic approach was modified to include additional variables, but these two basic geometrical values remained at the heart of all NACA aerofoil series, as illustrated below.

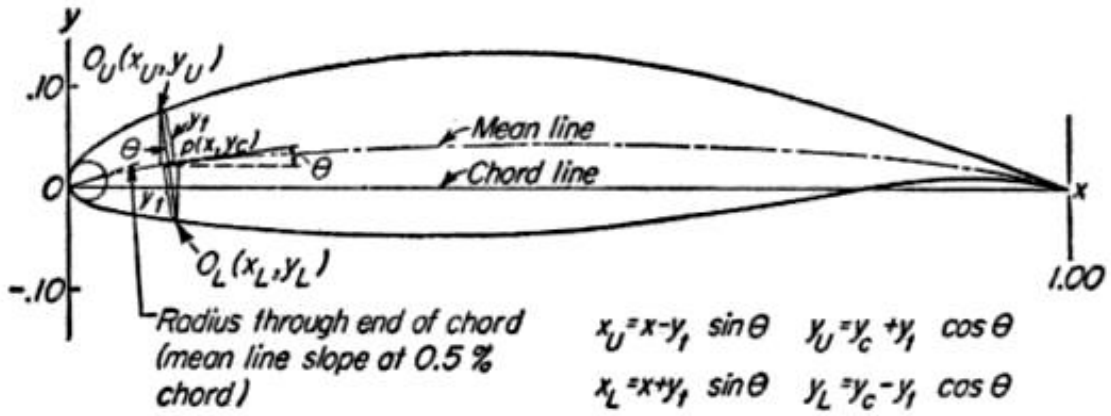

Fig1.6 NACA Aerofoil Geometrical Construction

1.7.1 NACA Four-Digit Series:

The first family of aerofoils designed using this approach became known as the NACA Four-Digit Series and represented as "mpxy".

The 1st digit 'm' specifies the maximum camber in percentage of the chord,

The second digit 'p' indicates the position of the maximum camber in terms of chord and

The last two digits 'xy' provide the maximum thickness of the aerofoil in percentage of chord.

For example: the NACA 2415 aerofoil has a maximum thickness of 15% with a camber of 2% located 40% back from the aerofoil leading edge.

1.8 OBJECTIVE OF THE WORK

To analyse symmetric and asymmetric aerofoils which is design using CATIA, to examine their velocity and surface pressure distribution using ANSYS by determining their drag and lift coefficients at various angle of attack and Mach number.

CHAPTER 2

LITERATURE REVIEW

NOVEL KUMAR SAHU & MR. SHADAB IMAM (2015) [1] have carried out a simulation analysis for a transonic flow over an aerofoil to give appropriate results which can further add scope of work for extended research. They have carried out the analysis in order to reduce tragic failures due to shock wave generation. Their results show that the strength of a shock wave increases with increase in Mach speed of the foil which also leads to increase in drag, both due to the emergence of wave drag, and also because the pressure rise through a shock wave thickens the boundary layer leading to increased viscous drag which limits the cruise speed. They suggested that usage of swept wings may reduce the drag up to some extent at high Mach speeds and the Mach induced changes in control effectiveness. They further added that increase in angle of attack results in increase of lift coefficient upto a limiting point after which an aerodynamic stall occurs. They finally concluded by stating the results that the limiting angle of attack is 16˚ after which the foil is observed to be stalled.

M. ARVIND (2010) [4] researched on NACA 4412 aerofoil and analysed its profile for consideration of an airplane wing .The NACA 4412 aerofoil was created using CATIA V5 And analysis was carried out using commercial code ANSYS 13.0 FLUENT at an speed of 340.29 m/sec for angles of attack of 0˚, 6˚, 12˚ and 16˚. k-ε turbulence model was assumed for Airflow. Fluctuations of static pressure and dynamic pressure are plotted in form of filled contour.

MAYURKYMAR KEVADIYA (2013) [7] studied the NACA 4412 aerofoil profile and recognized its importance for investigation of wind turbine edge. Geometry of the aerofoil is made utilizing GAMBIT 2.4.6. Also CFD investigation is done utilizing FLUENT 6.3.26 at different approaches from 0˚to 12˚

P. SETHUNATHA, M. NIVENTHRAN, V. SIVA & R. SADHAN KUMAR [5] have carried out an analysis on different supercritical aerofoils like NACA 0406, 0412, 0706 and 1006 to show the improvement in the climbing performance of the foils at subsonic Mach speeds. He showed that a cusp like structure at the trailing

edge of an unsymmetrical aerofoil produces a very high improvement in climbing performance. The test is carried out at a subsonic speed of around 25m/s and the results so obtained show the reduction in drag and improvement in coefficient of lift by 15-20% when compared with baseline model.

CHARLES H. CARLSON (1983) [8], This paper aims at the development of the scram jet propulsion system for HYSAM is based upon previous Marquardt experience. Technology gained from previous full scale engine development programs established the combustion cycle logic. The data consists of analytical and experimental results from direct connect and free jet engine tests simulating a free stream Mach number of 5.92.

N. AHMED ET AL. (1998) [9] contemplated the numerical reproduction of stream past aerofoils is vital in the flight optimized outline of air ship wings and turbo-hardware parts. These lifting gadgets regularly achieve ideal execution at the state of onset of partition. Hence, division phenomena must be incorporated if the examination is gone for pragmatic applications. Thus, in the present study, numerical recreation of relentless stream in a straight course of NACA 0012 aerofoils is expert with control volume approach.

D. RANA, S. PATEL, AK. ONKAR & M. MANJUPRASAD (2009) [10] studied the flutter characteristics of an aerofoil in a 2-D subsonic flow by using RANS based CFD solver with a structural code in time domain .

MOCHAMMAD AGOES MOELYADI (2002) [2] has done the trailing edge modifications by employing different wedge profiles. He has carried out simulation for RAE 2822 transonic aerofoil by changing the wedge shapes at the aft portion of the foil. He has taken two different wedge configurations where he has changed the length to height ratios and concluded by saying that the aerofoil with wedge having a length of 1% of the chord and height equal to 0.5% is giving good aerodynamic performance in comparison with foil with other wedge profiles. The six different wedge profiles under two configurations ratio wise for which the experiments were conducted.

SANJAY GOEL (2008) [6] devised a method of optimization of Turbine Aerofoil using Quansi – 3D analysis codes. He solved the complexity of 3D modelling by

modelling multiple 2D aerofoil sections and joining their figure in radial direction using second and first order polynomials that leads to no roughness in the radial direction.

T. GULTOP (1995) [3] studied the impact of perspective degree on Aerofoil performance. The reason for this study was to focus the ripple conditions not to be kept up throughout wind tunnel tests. These studies indicate that aero elastic insecurities for the changing arrangements acknowledged showed up at Mach number 0.55, which was higher than the wind tunnel Mach number point of confinement velocity of 0.3.

CHAPTER 3

DESIGNING & MODELLING

There are many software's available to model aerofoil profiles like CREO, SOLIDWORKS, INVENTOR, CATIA etc. But based on our requirement, we have made use of CATIA for designing NACA 0015 and NACA 6409.

3.1 CATIA HISTORY

CATIA started as an in-house development in 1977 by French aircraft manufacturer Avions Marcel Davot at that time customer of the CADAM software to develop Dassault's Mirage fighter jet. It was later adopted by the aerospace, automotive, shipbuilding, and other industries.

Initially named CATI (conception assistée tridimensionnelle interactive – French for interactive aided three-dimensional design), it was renamed CATIA in 1981 when Dassault created a subsidiary to develop and sell the software and signed a non-exclusive distribution agreement with IBM.

3.2 SCOPE OF CATIA

Commonly referred to as a 3D Product lifecycle management software suite, CATIA supports multiple stages of product development (CAx), including conceptualization, design (CAD) engineering (CAE) and manufacturing (CAM). CATIA facilitates collaborative engineering across disciplines around its 3DEXPERIENCE platform, including surfacing & shape design, electrical, fluid and electronic systems design mechanical engineering and systems engineering.

CATIA facilitates the design of electronic, electrical, and distributed systems such as fluid and HVAC systems, all the way to the production of documentation for manufacturing.

3.3 DESIGNING PROCEDURE

- Open the aerofoil plots of NACA 0015 **[1]** and then copy its coordinates.
- Then select program files in 'C Drive', then select Dassault systems →B27 → winb64 → code→ command, and open select GSD point spline loft from excel to paste the coordinates.
- To create space between the coordinates, click on 'data' and then on 'text on columns' then select 'space' and click OK.
- Then convert the coordinates from metres to millimetres and define 3rd coordinate.

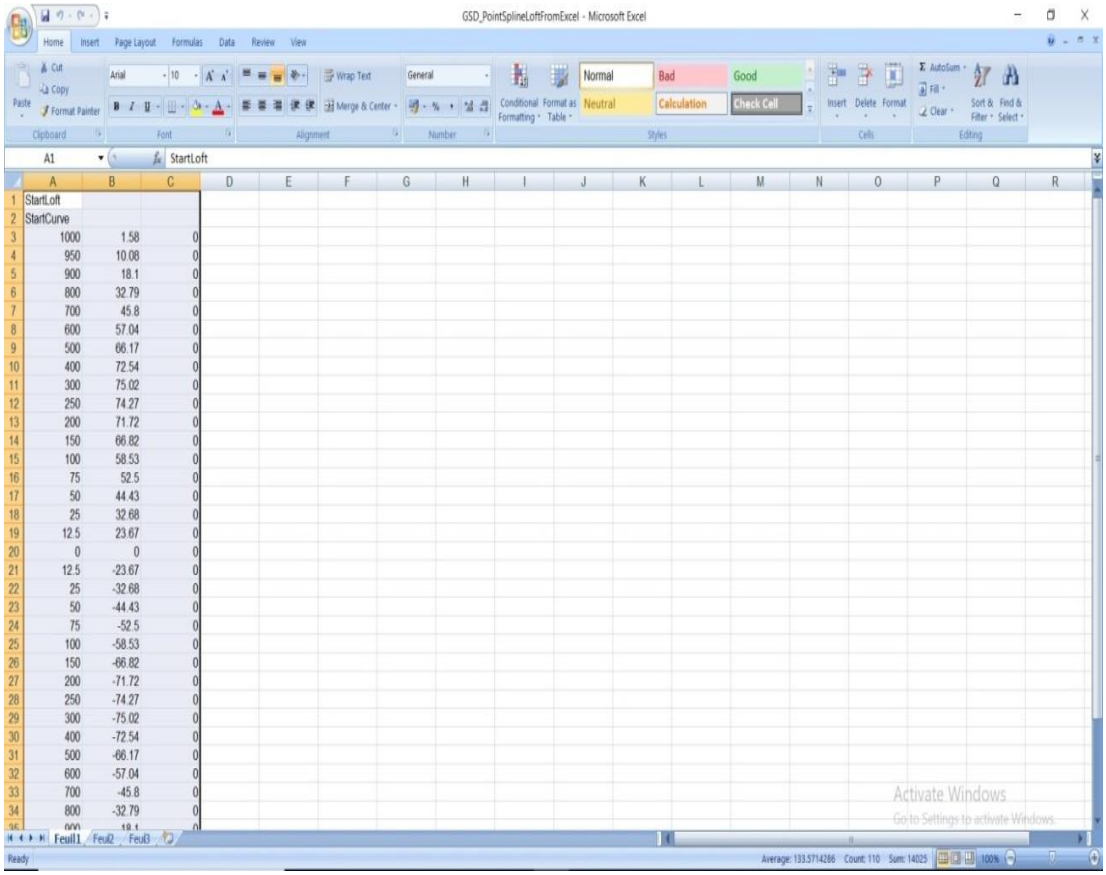

Fig 3.1 : Excel Coordinates

- Then enable all the macros in macro settings and then save and close it.
- Then open CATIA and select start, then mechanical design and then select wire rame modelling.
- Again go to Excel sheet, select macros in view then select GSD point spline off from Excel and then run it and type 1 to complete the plotting in CATIA.
- Now coordinates are defined in CATIA, so select XY plane and select sketcher to draw vertical line.

- Then select all the points and click on Insert → Operations → 3D geometry → Project 3D elements and then on OK to define the object.
- Then select Insert → Operation→ Transformation → Mirror, to obtain Mirror of the required Profile.
- Then delete the Right side Coordinates and exit work bench geometry from Excel and then delete it.
- Then Double click on Vertical Line and select all the Coordinates to mirror it then delete the Previous Coordinates and the vertical line.
- Then select Spline to join the coordinates and then Exit the workbench.
- Now click on fill and select 2 curves to fill the profile and then press OK and save it as IGS file.
- Then close Window.
- Similiarly design NACA 6409 by following above procedure.

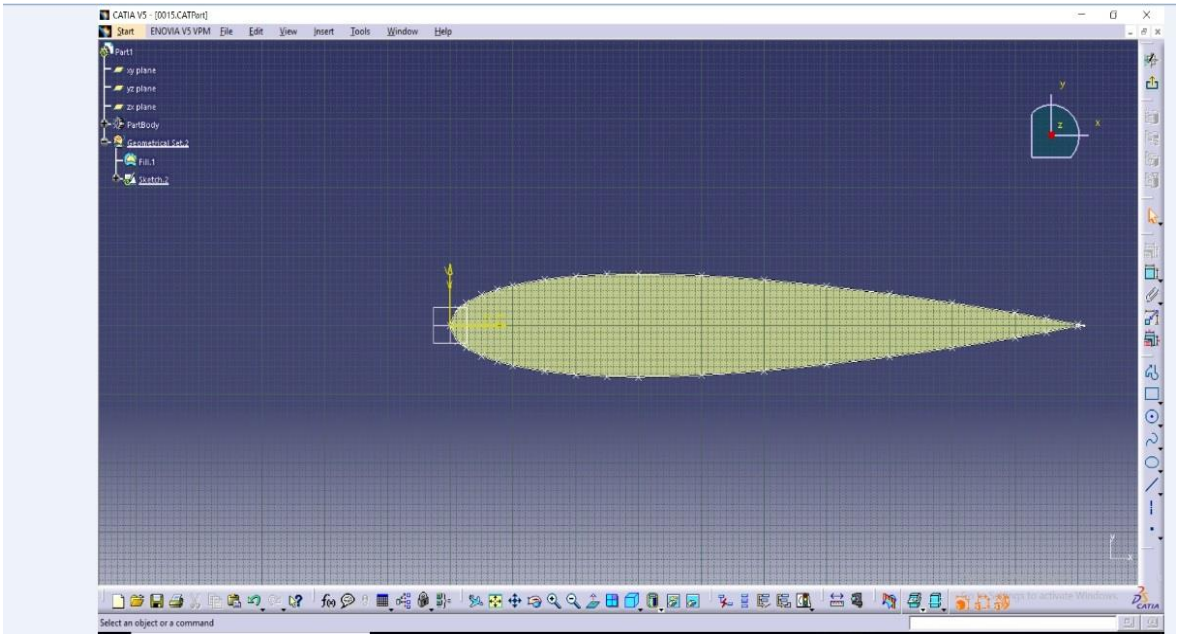

Fig 3.2 : Aerofoil Profile

CHAPTER 4

COMPUTATIONAL FLUID DYNAMICS

4.1 CFD

CFD is one of the branches of fluid mechanics that uses numerical methods and algorithms to solve and analyze problems that involve fluid flows. Computers are used to perform the millions of calculations required to simulate the interaction of fluids and gases with the complex surfaces used in engineering. However, even with simplified equations and high speed supercomputers, only approximate solutions can be achieved in many cases. More accurate codes that can accurately and quickly simulate even complex scenarios such as supersonic or turbulent flows are an ongoing area of research.

4.2 GOVERNING EQUATIONS

The governing equations of fluid flow represent mathematical statements of the conservation laws of physics. Each individual governing equation represents a conservation principle. The fundamental equations of fluid dynamics are based on the following universal laws of conservation. They are,

Unsteady state 3-D equation of continuity:-

$$\frac{\partial \rho}{\partial t} + div(\rho u) = 0$$

Momentum equation:-

$$\frac{\partial(\rho u)}{\partial t} + div\,(\rho u \mu) = -\frac{\partial P}{\partial x} + div(\mu grad u)$$

Energy equation:-

$$\frac{\partial(\rho i)}{\partial t} + \mathrm{div}(\rho i u) = -P\,\mathrm{div}\,u + \mathrm{div}(k\,\mathrm{grad}\,T) + \emptyset + S$$

4.3 DISCRETISATION METHODS OF CFD

There are three discretization methods in CFD:

1. Finite difference method (FDM)

2. Finite volume method (FVM)

3. Finite element method (FEM)

4.3.1 Finite Difference Method (FDM)

A finite difference method (FDM) discretization is based upon the differential form of the PDE to be solved. Each derivative is replaced with an approximate difference formula (that can generally be derived from a Taylor series expansion). The computational domain is usually divided into hexahedral cells (the grid), and the solution will be obtained at each nodal point. The FDM is easiest to understand when the physical grid is Cartesian, but through the use of curvilinear transforms the method can be extended to domains that are not easily represented by brick-shaped elements. The Discretization results in a system of equation of the variable at nodal points, and once a solution is found, then we have a discrete representation of the solution.

4.3.2 Finite Volume Method (FVM)

A finite volume method (FVM) discretization is based upon an integral form of the PDE to be solved (e.g. conservation of mass, momentum, or energy). The PDE is written in a form which can be solved for a given finite volume (or cell). The computational domain is discretized into finite volumes and then for every volume the governing equations are solved. The resulting system of equations usually involves fluxes of the conserved variable, and thus the calculation of fluxes is very important in FVM. The basic advantage of this method over FDM is it does not require the use of structured grids, and the effort to convert the given mesh in to structured numerical grid internally is completely avoided. As with FDM, the resulting approximate solution is a discrete, but the variables are typically placed at cell canters rather than at nodal points. This is not always true, as there are also face-cantered finite volume methods. In any case, the values of field variables at non-storage locations (e.g. vertices) are obtained using interpolation.

4.3.3 Finite Element Method (FEM)

A finite element method (FEM) discretization is based upon a piecewise representation of the solution in terms of specified basis functions. The computational

domain is divided up into smaller domains (finite elements) and the solution in each element is constructed from the basic functions. The actual equations that are solved are typically obtained by restating the conservation equation in weak form: the field variables are written in terms of the basic functions; the equation is multiplied by appropriate test functions, and then integrated over an element. Since the FEM solution is in terms of specific basis functions, a great deal more is known about the solution than for either FDM or FVM. This can be a double-edged sword, as the choice of basic functions is very important and boundary conditions may be more difficult to formulate. Again, a system of equations is obtained (usually for nodal values) that must be solved to obtain a solution.

Comparison of the three methods is difficult, primarily due to the many variations of all three methods. FVM and FDM provide discrete solutions, while FEM provides a continuous (up to a point) solution. FVM and FDM are generally considered easier to program than FEM, but opinions vary on this point. FVM are generally expected to provide better conservation properties, but opinions vary on this point also.

4.4 WORKING OF CFD

CFD codes are structured around the numerical algorithms that can be tackle fluid problems. In order to provide easy access to their solving power all commercial CFD packages include sophisticated user interfaces input problem parameters and to examine the results. Hence all codes contain three main elements:

1. Pre-processing.

2. Solver

3. Post-processing.

4.4.1 Pre-Processing

This is the first step in building and analyzing a flow model. Pre-processor consist of input of a flow problem by means of an operator –friendly interface and subsequent transformation of this input into form of suitable for the use by the solver. The user activities at the Pre-processing stage involve:

- Definition of the geometry of the region: The computational domain.
- Grid generation the subdivision of the domain into a number of smaller, non overlapping sub domains (or control volumes or elements Selection of physical or chemical phenomena that need to be modelled).

- Definition of fluid properties
- Specification of appropriate boundary conditions at cells, which coincide with or touch the boundary. The solution of a flow problem (velocity, pressure, temperature etc.) is defined at nodes inside each cell. The accuracy of CFD solutions is governed by number of cells in the grid. In general, the larger numbers of cells better the solution accuracy. Both the accuracy of the solution & its cost in terms of necessary computer hardware & calculation time are dependent on the fineness of the grid. Efforts are underway to develop CFD codes with a (self) adaptive meshing capability. Ultimately such programs will automatically refine the grid in areas of rapid variation.

4.4.2 Solver

The CFD solver does the flow calculations and produces the results. FLUENT, FloWizard, FIDAP, CFX and POLYFLOW are some of the types of solvers.

FLUENT is used in most industries. FloWizard is the first general-purpose rapid flow modelling tool for design and process engineers built by Fluent. POLYFLOW (and FIDAP) are also used in a wide range of fields, with emphasis on the materials processing industries. FLUENT and CFX two solvers were developed independently by ANSYS and have a number of things in common, but they also have some significant differences. Both are control-volume based for high accuracy and rely heavily on a pressure-based solution technique for broad applicability. They differ mainly in the way they integrate the fluid flow equations and in their equation solution strategies. The CFX solver uses finite elements (cell vertex numerics), similar to those used in mechanical analysis, to discretize the domain. In contrast, the FLUENT solver uses finite volumes (cell centred numerics). CFX software focuses on one approach to solve the governing equations of motion (coupled algebraic multi grid), while the FLUENT product offers several solution approaches (density, segregated- and coupled-pressure-based methods)

Properties of Solver

The FLUENT CFD code has extensive interactivity, so we can make changes to the analysis at any time during the process. This saves time and enables to refine designs more efficiently. Graphical user interface (GUI) is intuitive, which helps to shorten the learning curve and make the modelling process faster. In addition, FLUENT's adaptive and dynamic mesh capability is unique and works with a wide range of physical models. This capability makes it possible and simple to model complex

moving objects in relation to flow. This solver provides the broadest range of rigorous physical models that have been validated against industrial scale applications, so we can accurately simulate real-world conditions, including multiphase flows, reacting flows, rotating equipment, moving and deforming objects, turbulence, radiation, acoustics and dynamic meshing. The FLUENT solver has repeatedly proven to be fast and reliable for a wide range of CFD applications. The speed to solution is faster because suite of software enables us to stay within one interface from geometry building through the solution process, to post-processing and final output.

The numerical solution of Navier–Stokes equations in CFD codes usually implies a discretization method: it means that derivatives in partial differential equations are approximated by algebraic expressions which can be alternatively obtained by means of the finite-difference or the finite-element method. Otherwise, in a way that is completely different from the previous one, the discretization equations can be derived from the integral form of the conservation equations: this approach, known as the finite volume method, is implemented in FLUENT, because of its adaptability to a wide variety of grid structures. The result is a set of algebraic equations through which mass, momentum, and energy transport are predicted at discrete points in the domain. In the freeboard model that is being described, the segregated solver has been chosen so the governing equations are solved sequentially. Because the governing equations are non-linear and coupled, several iterations of the solution loop must be performed before a converged solution is obtained and each of the iteration is carried out as follows:

(1) Fluid properties are updated in relation to the current solution; if the calculation is at the first iteration, the fluid properties are updated consistent with the initialized solution.

(2) The three momentum equations are solved consecutively using the current value for pressure so as to update the velocity field.

(3) Since the velocities obtained in the previous step may not satisfy the continuity equation, one more equation for the pressure correction is derived from the continuity equation and the linearized momentum equations: once solved, it gives the correct pressure so that continuity is satisfied. The pressure–velocity coupling is made by the SIMPLE algorithm, as in FLUENT default options.

(4) Other equations for scalar quantities such as turbulence, chemical species and radiation are solved using the previously updated value of the other variables; when inter-phase coupling is to be considered, the source terms in the appropriate

continuous phase equations have to be updated with a discrete phase trajectory calculation.

(5) Finally, the convergence of the equations set is checked and all the procedure is repeated until convergence criteria are met.

4.4.3 Post-Processing:

This is the final step in CFD analysis, and it involves the organization and interpretation of the predicted flow data and the production of CFD images and animations. Fluent's software includes full post processing capabilities. FLUENT exports CFD's data to third-party post-processors and visualization tools such as Ensight, Fieldview and TechPlot as well as to VRML formats. In addition, FLUENT CFD solutions are easily coupled with structural codes such as ABAQUS, MSC and ANSYS, as well as to other engineering process simulation tools.

Thus FLUENT is general-purpose computational fluid dynamics (CFD) software ideally suited for incompressible and mildly compressible flows. Utilizing a pressure-based segregated finite-volume method solver, FLUENT contains physical models for a wide range of applications including turbulent flows, heat transfer, reacting flows, chemical mixing, combustion, and multiphase flows. FLUENT provides physical models on unstructured meshes, bringing you the benefits of easier problem setup and greater accuracy using solution-adaptation of the mesh. FLUENT is a computational fluid dynamics (CFD) software package to simulate fluid flow problems. It uses the finite-volume method to solve the governing equations for a fluid. It provides the capability to use different physical models such as incompressible or compressible, inviscid or viscous, laminar or turbulent, etc.

Geometry and grid generation is done using GAMBIT which is the pre-processor bundled with FLUENT. Owing to increased popularity of engineering work stations, many of which has outstanding graphics capabilities, the leading CFD are now equipped with versatile data visualization tools. These include : Domain geometry & Grid display ,Vector plots, Line & shaded contour plots, 2D & 3D surface plots, Particle tracking, View manipulation (translation, rotation, scaling etc).

4.5 ADVANTAGES

- No restriction to linearity.
- Complicated physics can be treated.
- Time evaluation of flow can be obtained.

- It has the potential of providing information not available by other means.
- Computational investigation can be performed with remarkable speed. Designer can study the implications of hundreds of different configurations in minimum time and choose the optimum design.
- It gives detailed and complete information. It can provide the values of all the relevant variables (pressure, velocity, temperature, concentration, turbulence) throughout the domain of interest.

Because of the above advantages, CFD tool is widely used for computational purpose. Therefore, we have made use of CFD for analysing the aerofoil profile.

4.6 APPLICATIONS OF CFD

- Aerodynamics of aircraft & Space vehicles: lift & drag
- Hydrodynamics of ships
- Weather prediction.

4.7 PREDICTING THE TURBULENT VISCOSITY

The following models can be used to predict the turbulent viscosity:

- Mixing length model.
- Spalart-Allmaras model.
- Standard *k*-ε model.
- *k*-ε RNG model.
- Realizable *k*-ε model.
- *k*-ω model.

4.7.1 The *k*-ε model

- K-epsilon (k-ε) turbulence model is the most common model used in Computational Fluid Dynamics (CFD) to simulate mean flow characteristics for turbulent flow conditions. It is a two equation model which gives a general description of turbulence by means of two transport equations (PDEs).

- For turbulent kinetic energy k,

$$\frac{\partial(\rho k)}{\partial t} + \frac{\partial(\rho k u_i)}{\partial x_i} = \frac{\partial}{\partial x_j}\left[\frac{\mu_t}{\sigma_k}\frac{\partial k}{\partial x_j}\right] + 2\mu_t E_{ij}E_{ij} - \rho\epsilon$$

- For dissipation ε,

$$\frac{\partial(\rho\epsilon)}{\partial t}+\frac{\partial(\rho\epsilon u_i)}{\partial x_i}=\frac{\partial}{\partial x_j}\left[\frac{\mu_t}{\sigma_\epsilon}\frac{\partial\epsilon}{\partial x_j}\right]+C_{1\epsilon}\frac{\epsilon}{k}2\mu_t E_{ij}E_{ij}-C_{2\epsilon}\rho\frac{\epsilon^2}{k}$$

(Rate of change of k or ε + Transport of k or ε by convection)= (Transport of k or ε by diffusion + Rate of production of k or ε - Rate of destruction of k or ε)

Where,

u_i represents velocity component in corresponding direction

E_{ij} represents component of rate of deformation

μ_t represents eddy viscosity

$$\mu_t=\rho C_\mu\frac{k^2}{\epsilon}$$

The equations also consist of some adjustable constants σ_k , σ_ϵ , $C_{1\epsilon}$ and $C_{2\epsilon}$. The values of these constants have been arrived at by numerous iterations of data fitting for a wide range of turbulent flows. These are as follows:

$C_\mu = 0.09$ $\sigma_k = 1.00$ $\sigma_\epsilon = 1.30$ $C_{1\epsilon} = 1.44$ $C_{2\epsilon} = 1.92$

4.8 PROCEDURE FOR ANALYSIS IN WORKBENCH

4.8.1 GENERATION OF DOMAIN

- Select fluid flow(FLUENT) → Geometry(browse) → Input , to input IGS file then select geometry to edit the geometry of aerofoil , then click on Import generate to generate the aerofoil .
- Now select sketcher in XY plane to draw circle on horizontal axis and constraints as coincident, now select general in dimensions to define the diameter of circle as 5000.
- Next draw rectangle with dimensions 5000 as length and 10000 as breadth, then trim the unwanted circle in modify option.
- Then go to Modelling → concept → surface from sketches → apply → surface sketch 1 to generate the profile.

- Then go to create → Boolean → operation → subtract to generate the required profile, here target body is outer surface and tool body is aerofoil surface.
- Again select sketcher in XY plane to draw circle of 2500 diameter on horizontal axis, distance between centre of circle and vertical axis is 500.
- Now click on Modelling and select sketch 2 → concept → surface from sketches → operation → add frozen to surface sketch 2 to generate the required aerofoil profile.
- Then again click on sketcher to draw rectangle of height 2000 and breadth 10000, distance between horizontal axis and horizontal line is 1000 and distance between vertical axis and vertical line is 1300.
- Then select Modelling → sketch generate to generate the aerofoil profile as shown in fig 4.1, save it on desktop.

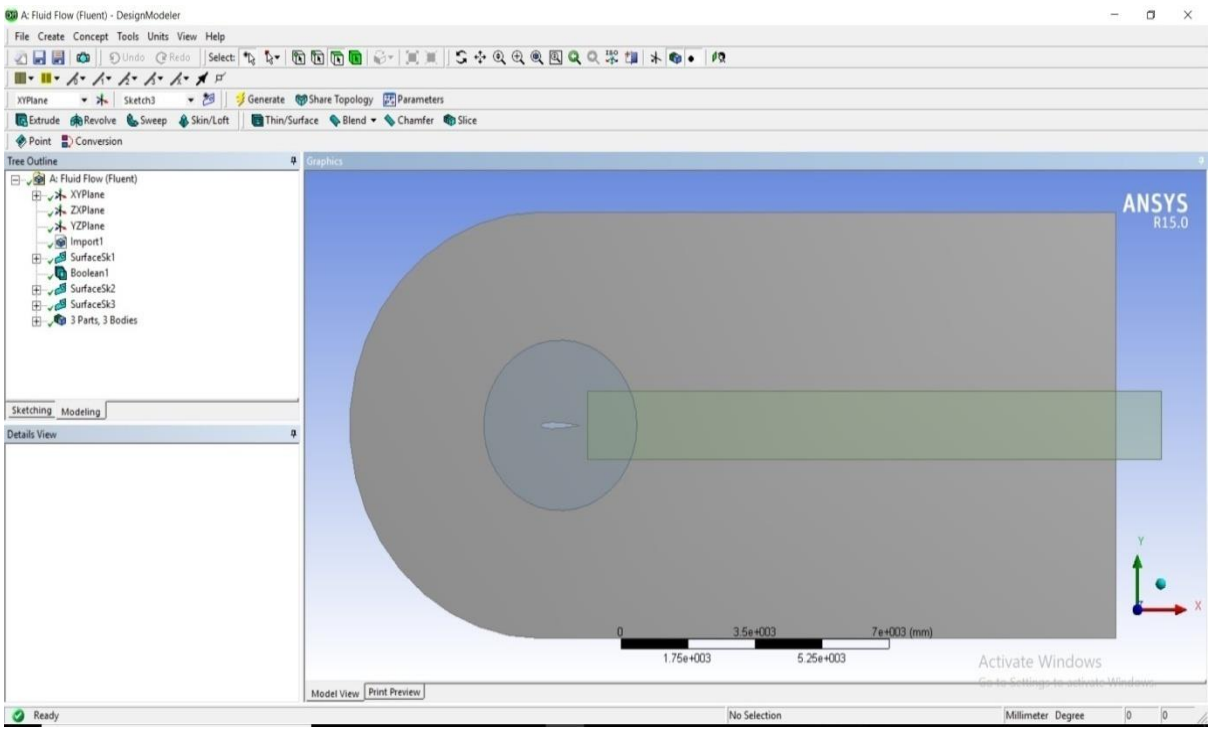

Fig4.1 Analysis In Workbench

4.8.2 MESHING

- For meshing go to mesh → edit , to edit the body
  Sizing: on proximity and curvature, Relevance: medium, Smoothening: high, Maximum face size: 0.4, Maximum size: 0.4.
- Then right click on mesh → insert →sizing ,and select

Scoping method: geometry selection (select outer body & apply) , Type : body of influence (select aerofoil bodies & apply) , then select element size as 0.3 .

- Again select mesh → insert → sizing, and select edge selection (aerofoil edges & apply), type: number of divisions, number of divisions =300 and behaviour as hard.
- Again go to mesh → insert → inflation → phase selection (select 2 boundary edges & apply) then select inflation option as total thickness, number of layers as 10 and maximum thickness as 0.1.
- Now go to connections → contacts → suppress to create name ,
  Select left edge → create name selection as inlet
  Select right edge → create name selection as outlet
  Select symmetric edges → create name selection as symmetric
  Select upper foil → create name selection as upper
  Select lower foil → create name selection as lower.
- Now go to mesh and click on generate to generate the mesh as shown in fig 4.2.

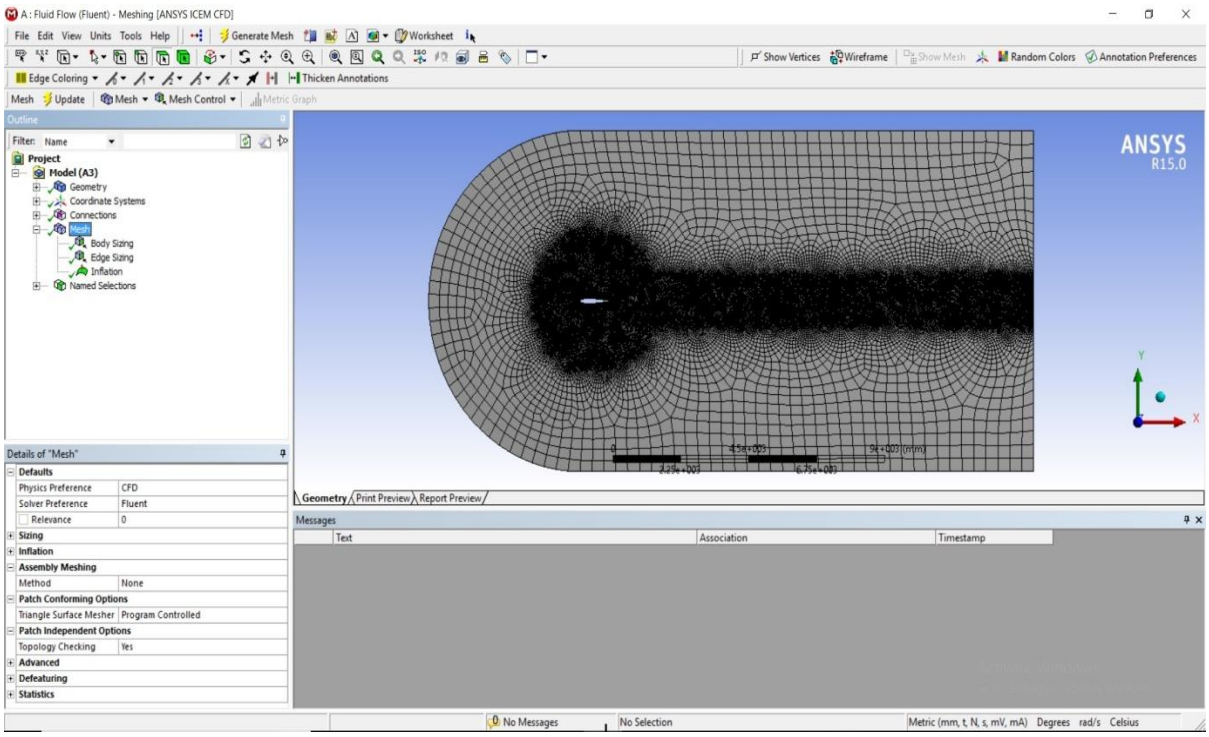

Fig4.2 Mesh Generation

4.8.3 SETUP

- Now go to edit →double precision →parallel → processor →OK.
- Then select general in solution setup

Type → density based
Model →energy on→equation →OK
lViscous →k-epsilon →OK
Material →fluid→density →idealgas→close
Cell zone conditions→ type →fluid →surface

Boundary conditions Inlet→ type→pressure far-field(enter Mach number& XY flow directions)

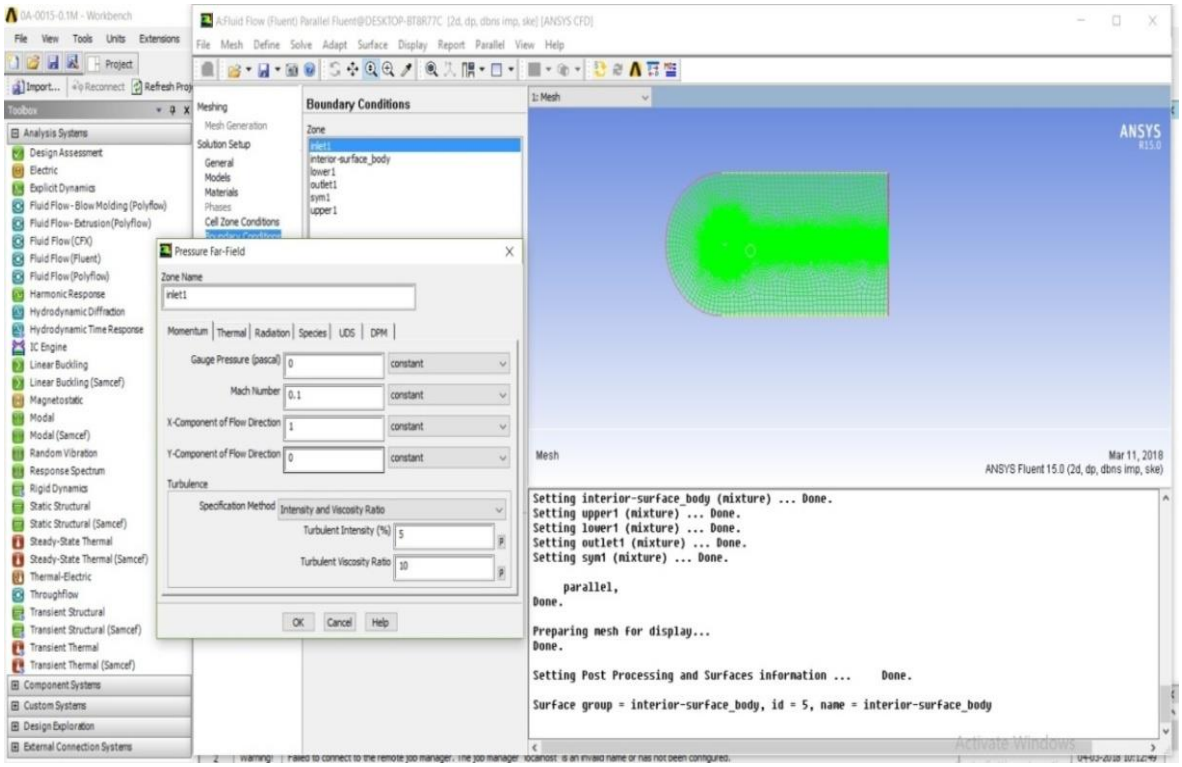

Fig4.3 Boundary Conditions

Lower→type→wall
Outlet →type→pressure outlet
Symmetric →type→symmetric
Upper →type→wall
Solution →monitors→create→drag, lift, momentum for plots .

- Then click on solve initialisation →standard solution.
- Then run solution and input Number of iterations as 2000 , then calculate as shown in figure 4.4.
- Now go to edit→use location →insert→contour→OK.
- Then select domain all→location symmetrical.
- Next click on variables→range→local→drag→contour .

- Similiarlly obtain the remaining plots.

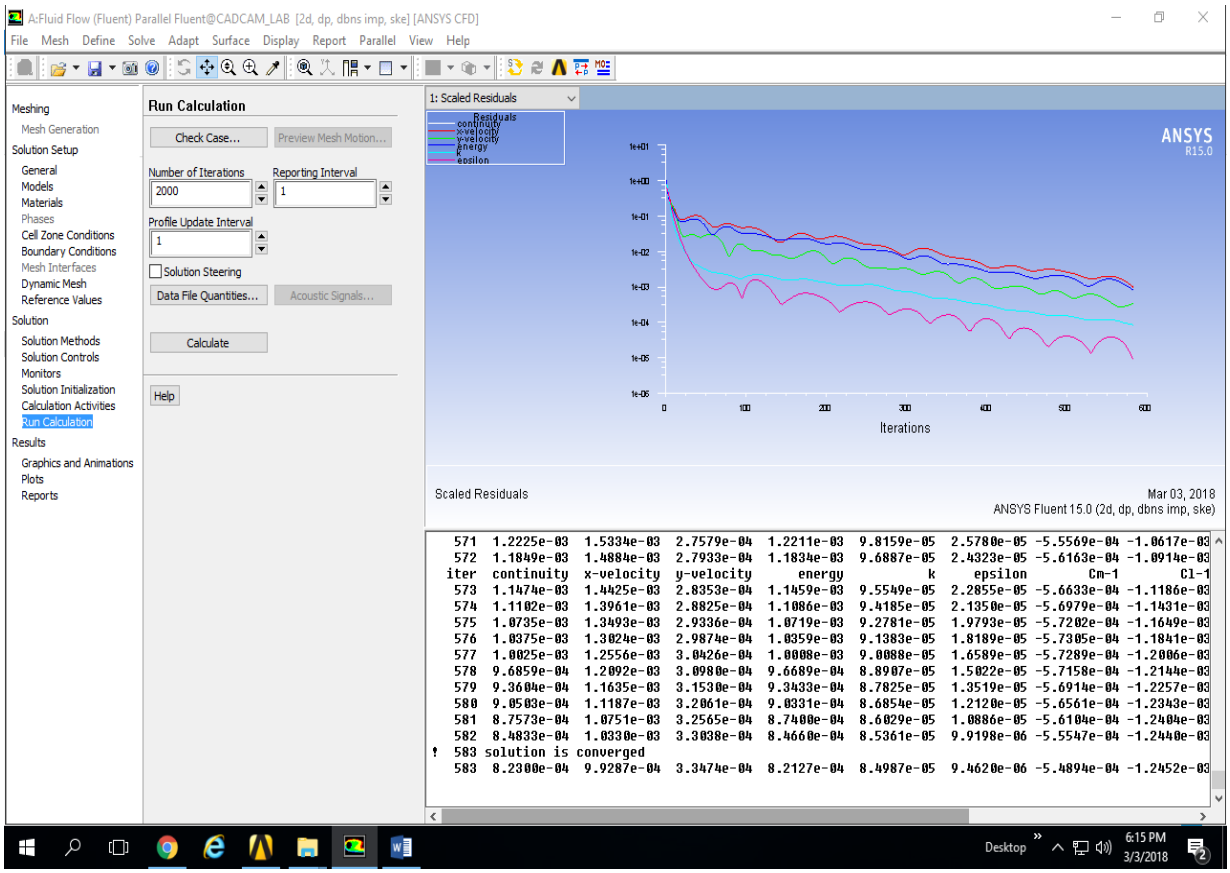

Fig4.4 Iterations

CHAPTER 5

RESULTS AND DISCUSSIONS

5.1 FOR NACA 0015

5.1.1 At Mach number 0.1

At angle of attack 0˚

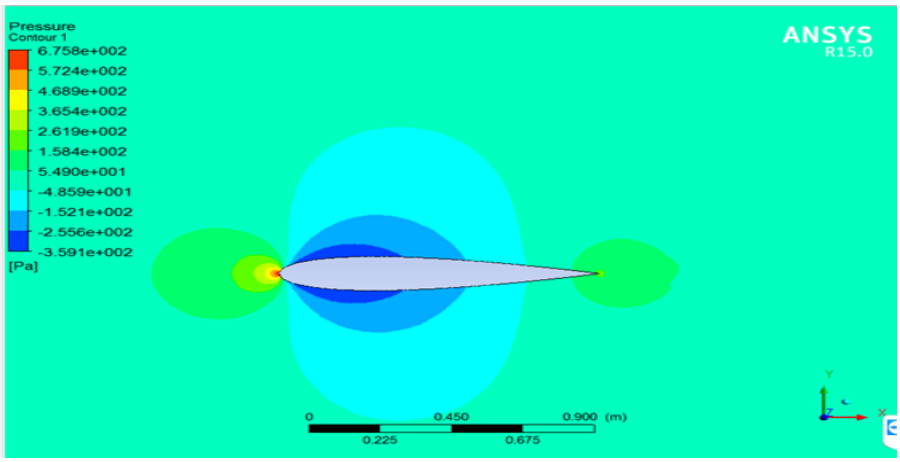

Fig5.1 Pressure Distribution for NACA 0015 at Mach number 0.1 and AOA 0˚

Referring to figure 5.1, it is clear that pressure at the leading edge is highest, significantly low in convex surfaces and varies moderately at trailing edge.

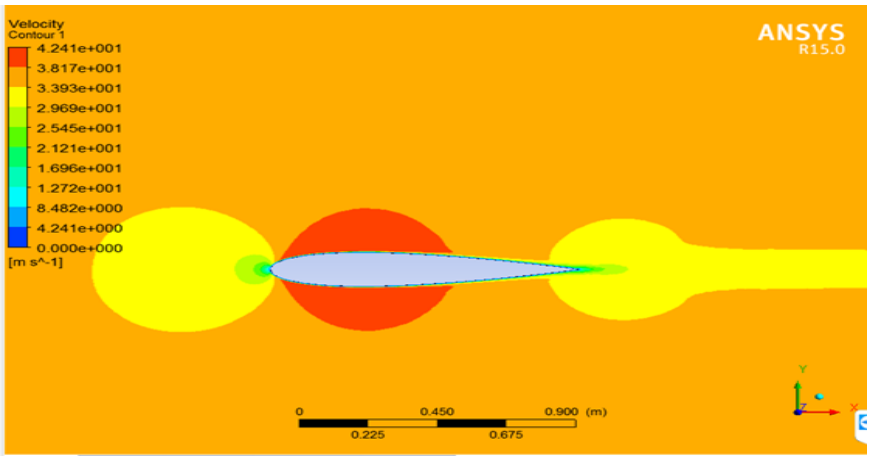

Fig5.2 Velocity Distribution for NACA 0015 at Mach number 0.1 and AOA 0˚

Referring to figure 5.2, from velocity contour 1, it is clear that velocity at the leading edge is lowest as pressure is highest, according to Bernoulli's principle. Similarly, velocity is more at convex surfaces and varies moderately at trailing edge.

5.1.2 At Mach number 0.4

At angle of attack 0°

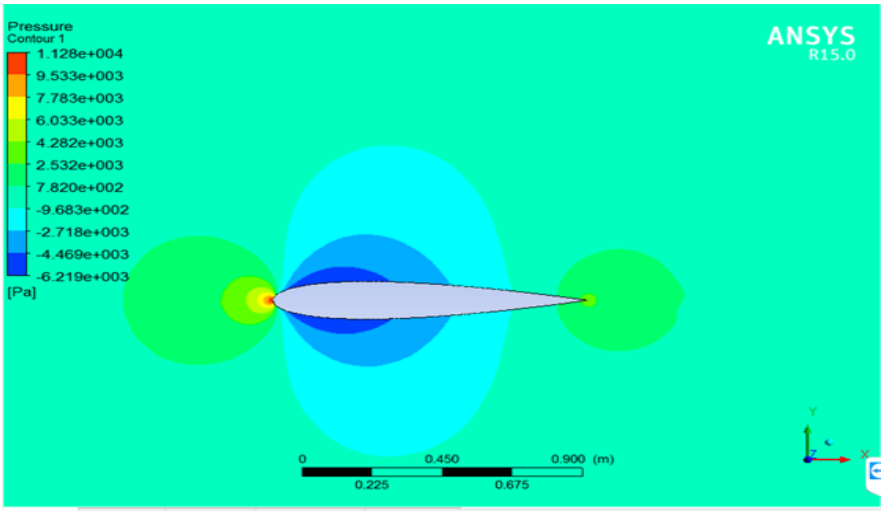

Fig5.3 Pressure Distribution for NACA 0015 at Mach number 0.4 and AOA 0˚

Referring to figure 5.3, at Mach number 0.4, we get higher pressure of 1.128e+004 at leading edge and lowest pressure of -6.219e+003 at convex surfaces.

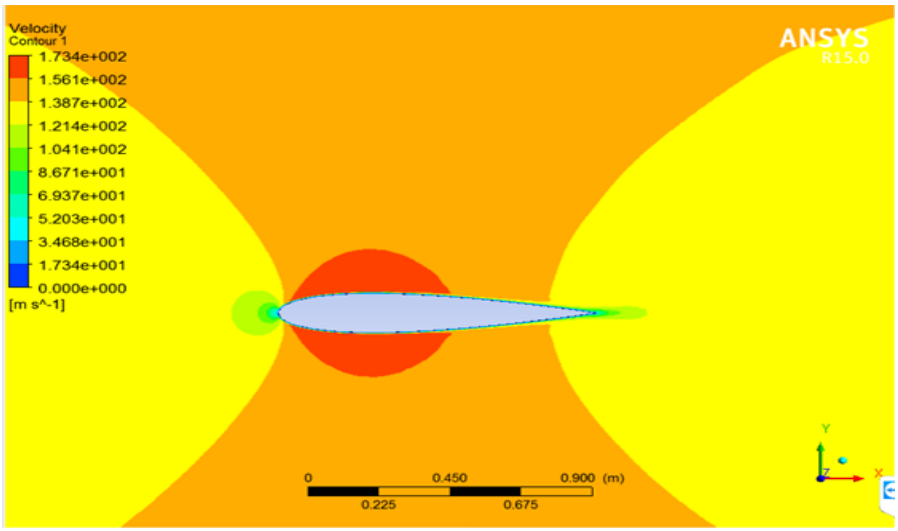

Fig5.4 Velocity Distribution for NACA 0015 at Mach number 0.4 and AOA 0˚

Refering to figure 5.4, at Mach number 0.4, the lowest velocity is 6.937e+001 at leading and trailing edge, and highest velocity is 1.734e+002 at convex surface of aerofoil i.e., higher value than velocity at Mach number 0.1.

5.2 FOR NACA 6409

5.2.1 At Mach number 0.1

At angle of attack 0˚

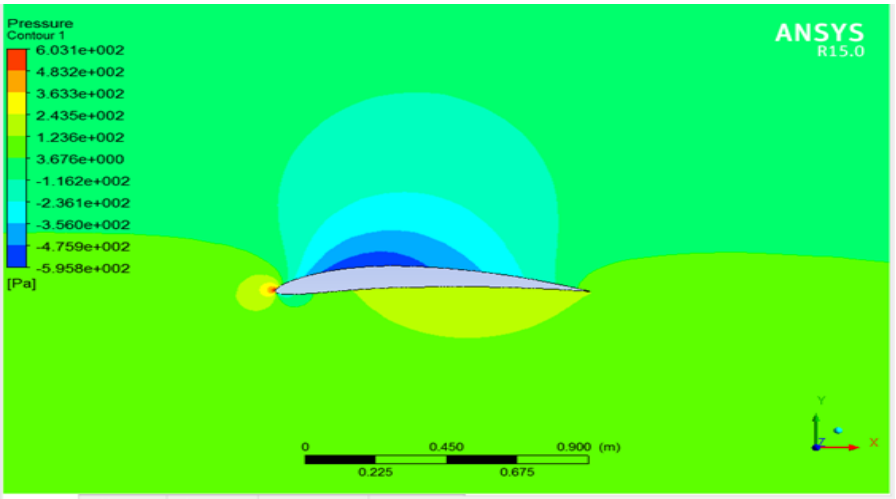

Fig5.5 Pressure Distribution for NACA 6409 at Mach number 0.1 and AOA 0˚

Referring to figure 5.5, from the pressure contour, we see that there is a region of high pressure at the leading edge (stagnation point) and region of varying low pressure at the upper surface of aerofoil.

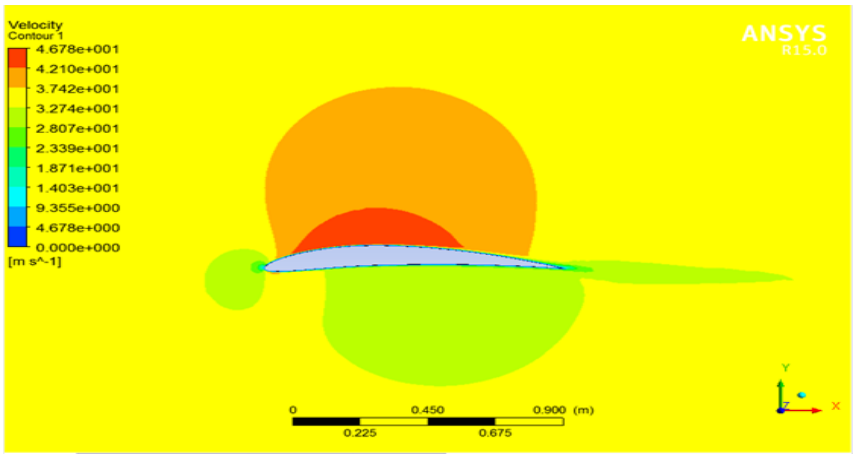

Fig5.6 Velocity Distribution for NACA 6409 at Mach number 0.1 and AOA 0˚

Referring to figure 5.6, from the velocity contour, we see that there is a region of high velocity at the convex surface, moderate velocity at the remaining surfaces.

5.2.2 At Mach number 0.4

At angle of attack 0°

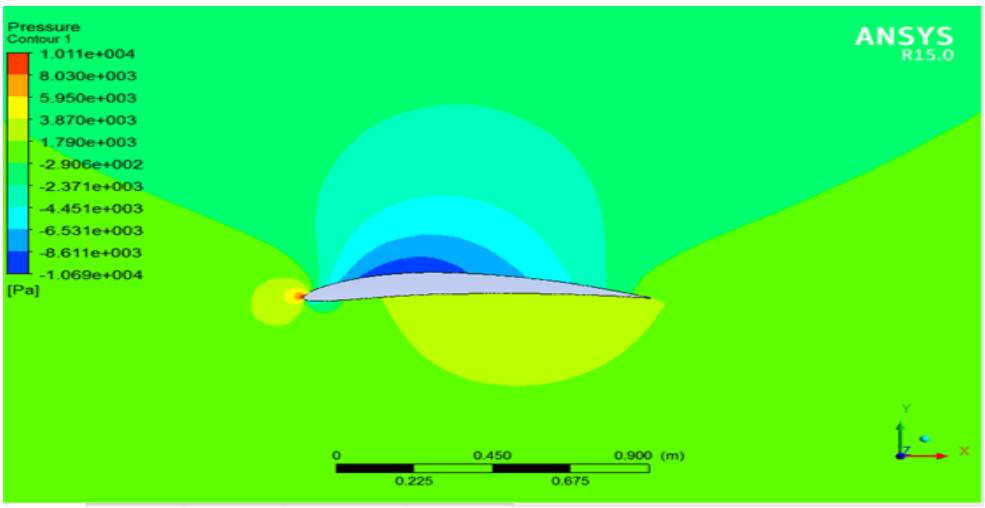

Fig5.7 Pressure Distribution for NACA 6409 at Mach number 0.4 and AOA 0˚

Referring to figure 5.7, at Mach number 0.4, we get higher pressure of 1.011e+004 at leading edge, lowest pressure of -1.069e+004 at convex surface and moderately varying at concave surface.

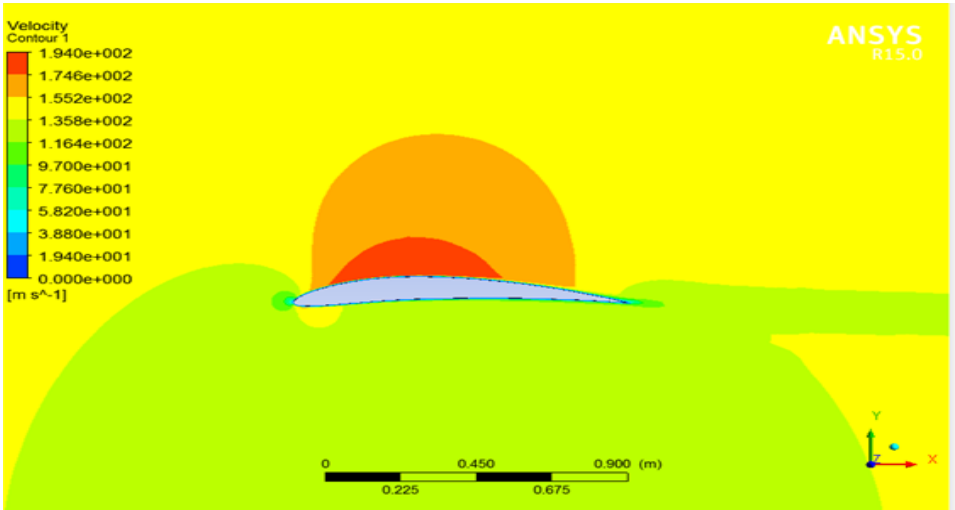

Fig5.8 Velocity Distribution for NACA 6409 at Mach number 0.4 and AOA 0˚

Referring to figure 5.8, at Mach number 0.4, the velocity of 9.700e+001 at leading edge, at trailing edge and at concave surface, and highest velocity is 1.940e+002 at convex surface of aerofoil i.e., higher value than velocity at Mach number 0.1.

5.3 PLOTS

5.3.1 C_d vs Angle of attack (AOA) at Mach number 0.1

Table 5.1 : C_d and AOA at Mach number 0.1

AOA	C_d symm	C_d asymm
-5	2.27E-02	-5.27E-03
0	1.05E-02	1.34E-02
5	2.27E-02	5.36E-02
10	5.53E-02	1.14E-01
15	1.04E-01	1.89E-01

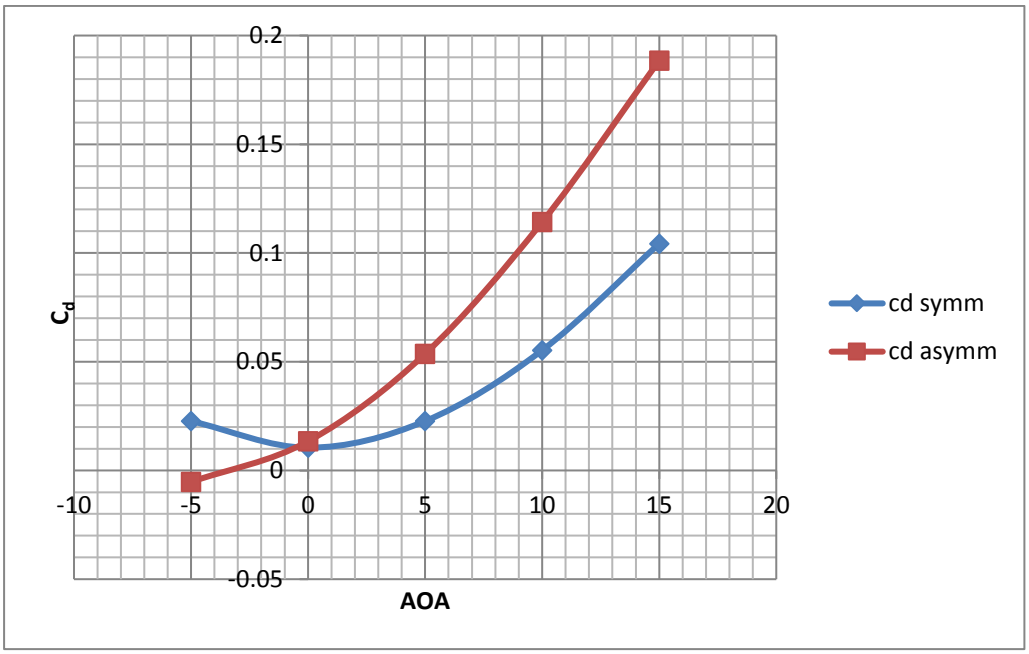

Fig5.9 C_d vs. AOA at Mach number 0.1

The graphical representation of the tabulated data of table 5.1 is shown in fig 5.9, The above figure represents **C_d** vs. AOA at Mach number 0.1 which shows comparison between symmetric and asymmetric aerofoil where coefficient of drag is taken on y axis and angle of attack is taken on x axis. It shows coefficient of drag increases with increase in angle of attack.

5.3.2 C_l vs. Angle of attack (AOA) at Mach number 0.1

Table 5.2: C_l and AOA at Mach number 0.1

AOA	C_l symm	C_l asymm
-5	2.60E-01	3.97E-01
0	-1.25E-03	6.56E-01
5	2.60E-01	9.15E-01
10	5.14E-01	1.14E+00
15	7.53E-01	1.34E+00

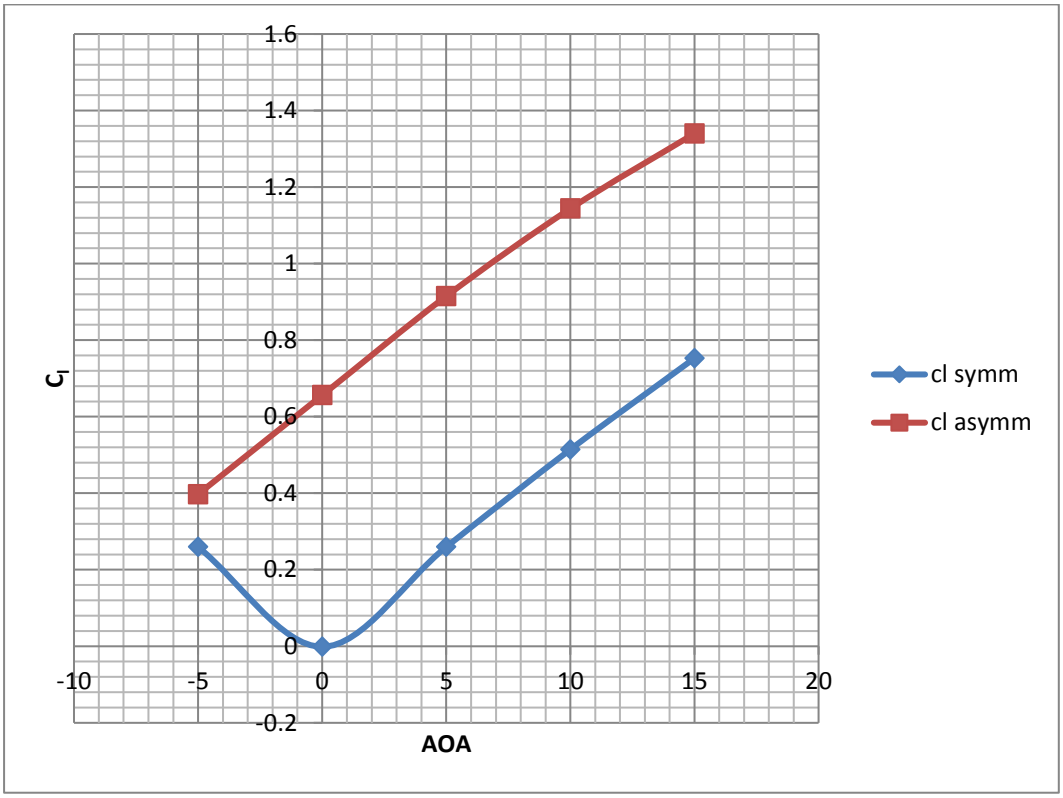

Fig5.10 C_l vs. AOA at Mach number 0.1

The graphical representation of the tabulated data of table 5.2 is shown in fig 5.10, The above figure represents C_l vs. AOA at Mach number 0.1 which shows comparison between symmetric and asymmetric aerofoil where coefficient of lift is taken on y axis and angle of attack is taken on x axis. It shows asymmetric aerofoil has higher coefficient of lift when compared to symmetric aerofoil.

5.3.3 C_m vs. Angle of attack (AOA) at Mach number 0.1

Table 5.3: C_m and AOA at Mach number 0.1

AOA	C_m symm	C_m asymm
-5	6.22E-02	2.51E-01
0	-5.49E-04	3.14E-01
5	6.22E-02	3.75E-01
10	1.23E-01	4.26E-01
15	1.76E-01	4.65E-01

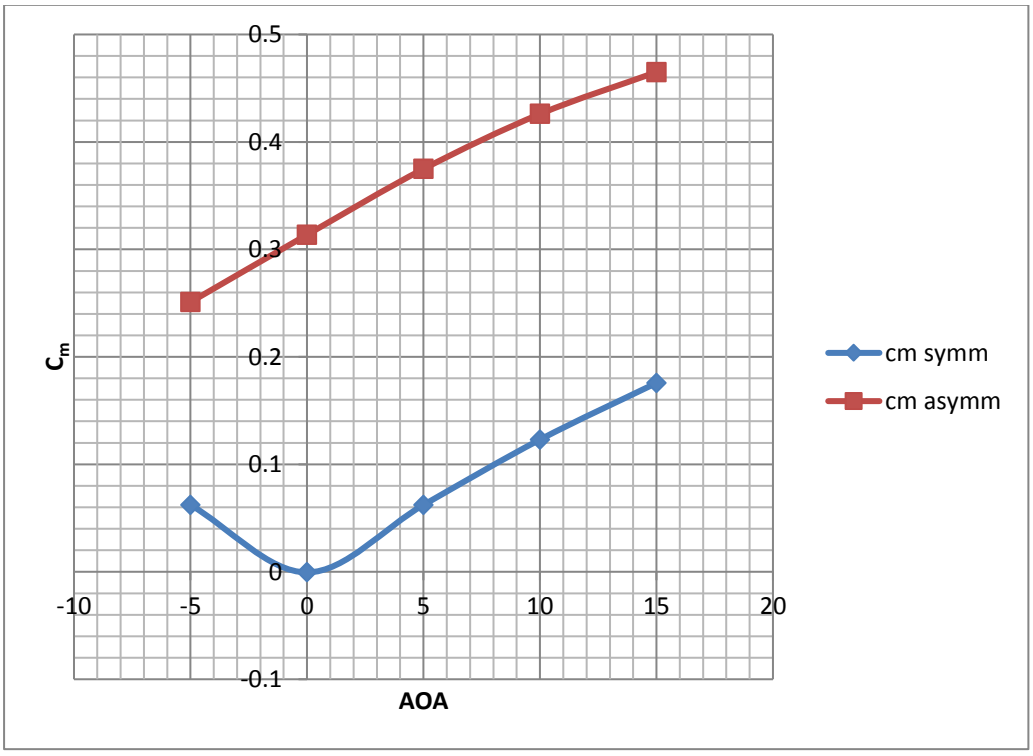

Fig 5.11 C_m vs. AOA at Mach number 0.1

The graphical representation of the tabulated data of table 5.3 is shown in fig 5.11, The above figure represents **C_m** vs. AOA at Mach number 0.1 which shows comparison between symmetric and asymmetric aerofoil where coefficient of pitching moment is taken on y axis and angle of attack is taken on x axis. It shows at zero angle of attack cm of symmetric aerofoil is zero whereas asymmetric aerofoil is greater than zero.

5.3.4 C_l / C_d vs. Angle of attack (AOA) at Mach number 0.1

Table 5.4: C_l / C_d and AOA at Mach number 0.1

AOA	C_l / C_d symm	C_l / C_d asymm
-5	1.42E+01	-76.654
0	-6.80E-02	56.45
5	1.42E+01	17.928
10	1.06E+01	10.544
15	7.81E+00	7.43

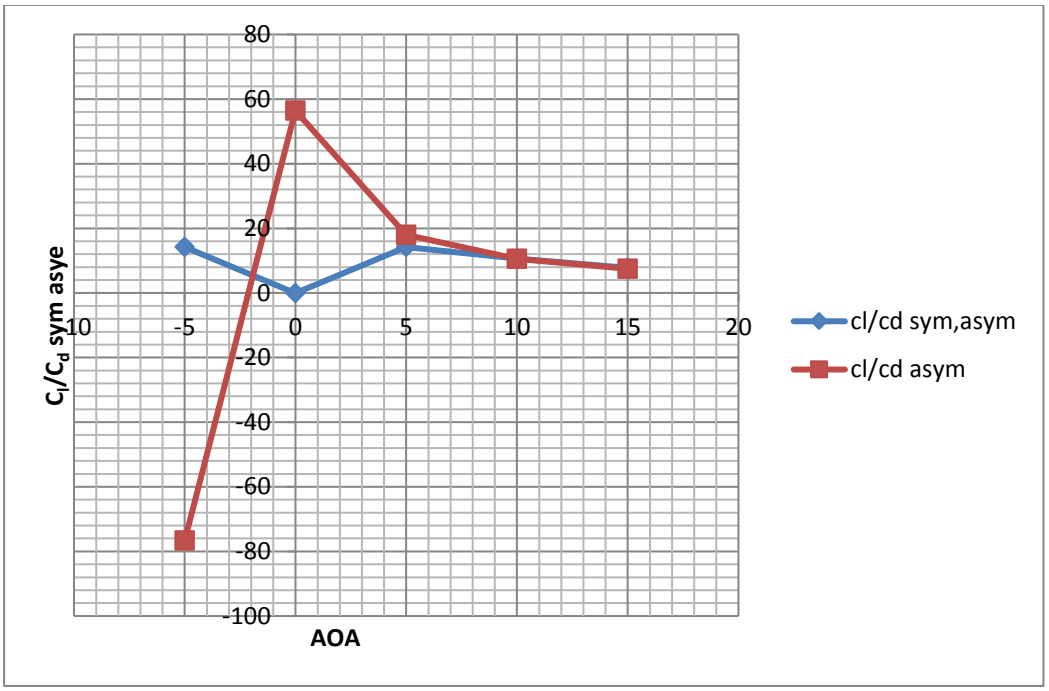

Fig No 5.12 C_l / C_d vs. AOA at Mach number 0.1

The graphical representation of the tabulated data of table5.4 is shown in fig 5.12, The above figure represents C_l / C_d vs. AOA at Mach number 0.1 which shows comparison between symmetric and asymmetric aerofoil where lift to drag ratio is taken on y axis and angle of attack is taken on x axis. Lift to drag ratio represents performance of aerofoil, hence above graph shows performance of asymmetric aerofoil is better than performance of symmetric aerofoil at zero AOA, vice versa at negative AOA and almost similar at positive AOA.

5.3.5 Cd vs. Angle of attack (AOA) at Mach number 0.4

Table 5.5: C_d and AOA at Mach number 0.4

AOA	C_d symm	C_d asymm
-5	2.10E-02	-5.44E-03
0	8.99E-03	1.27E-02
5	2.10E-02	5.63E-02
10	5.54E-02	1.21E-01
15	1.11E-01	2.03E-01

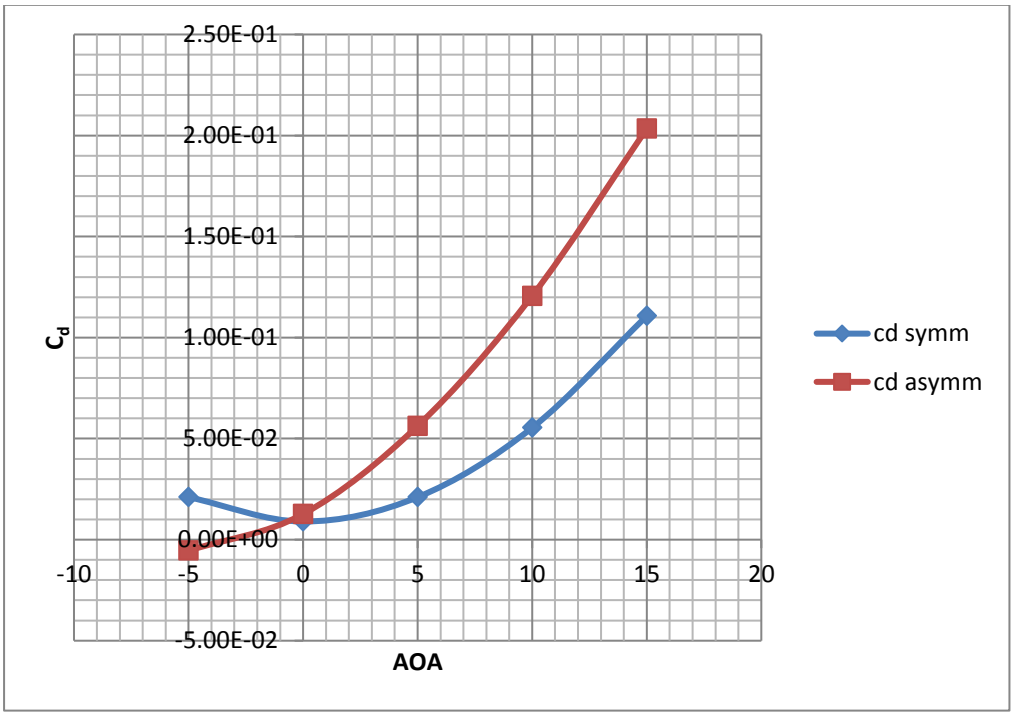

Fig 5.13 C_d vs. AOA at Mach number 0.4

The graphical representation of the tabulated data of table 5.5 is shown in fig 5.13, The above figure represents **C_d** vs. AOA at Mach number 0.4 which shows comparison between symmetric and asymmetric aerofoil where coefficient of drag is taken on y axis and angle of attack is taken on x axis. It shows coefficient of drag is less when compared to coefficient of drag at 0.1 Mach number.

5.3.6 C_l vs. Angle of attack (AOA) at Mach number 0.4

Table 5.6: C_l and AOA at Mach number 0.4

AOA	C_l symm	C_l asymm
-5	2.98E-01	4.17E-01
0	-6.18E-04	7.17E-01
5	2.98E-01	1.0094
10	5.90E-01	1.2759
15	8.67E-01	1.51

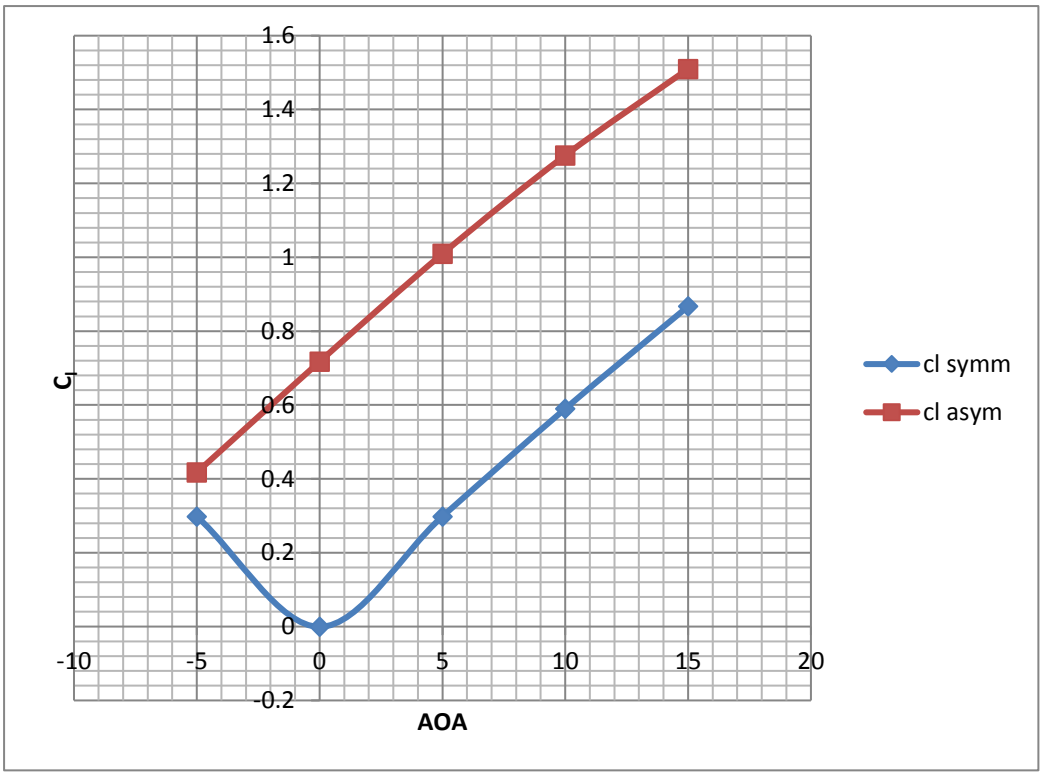

Fig 5.14 C_l vs. AOA at Mach number 0.4

The graphical representation of the tabulated data of table 5.6 is shown in fig 5.14, The above figure represents C_l vs. AOA at Mach number 0.4 which shows comparison between symmetric and asymmetric aerofoil where coefficient of lift is taken on y axis and angle of attack is taken on x axis. It shows asymmetric aerofoil has higher coefficient of lift when compared to symmetric aerofoil as well coefficient of lift of aerofoil at Mach number 0.4 is greater than coefficient of lift at Mach number 0.1.

5.3.7 C_m vs. Angle of attack (AOA) at Mach number 0.4

Table 5.7: C_m and AOA at Mach number 0.4

AOA	C_m symm	C_m asymm
-5	6.99E-02	2.71E-01
0	-4.49E-04	3.44E-01
5	6.99E-02	4.12E-01
10	1.37E-01	4.70E-01
15	1.98E-01	5.15E-01

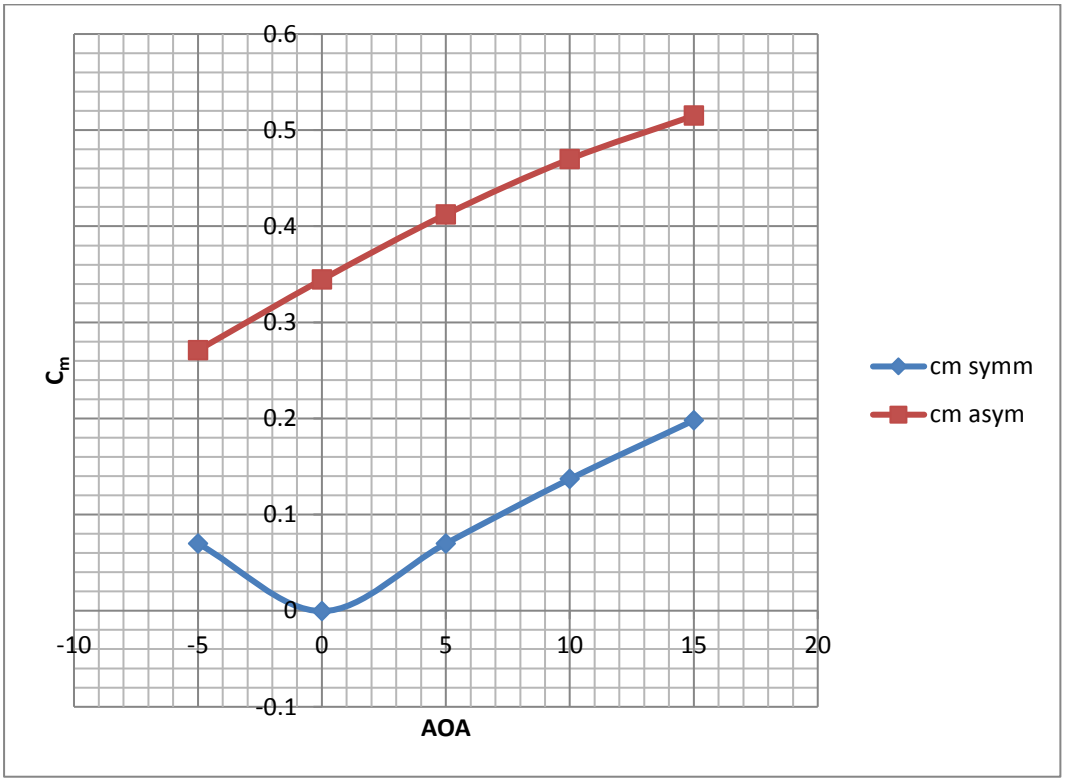

Fig 5.15 C_m vs. AOA at Mach number 0.4

The graphical representation of the tabulated data of table 5.7 is shown in fig 5.15, The above figure represents **C_m** vs. AOA at Mach number 0.4 which shows comparison between symmetric and asymmetric aerofoil where coefficient of pitching moment is taken on y axis and angle of attack is taken on x axis. It shows at zero angle of attack cm of symmetric aerofoil is zero whereas asymmetric aerofoil is greater than zero and coefficient pitching moment is less when compared to Mach number 0.1.

5.3.8 C_l / C_d vs. Angle of attack (AOA) at Mach number 0.4

Table 5.8: C_l / C_d vs. AOA at Mach number 0.4

AOA	C_l / C_d symm	C_l / C_d asymm
-5	1.42E+01	-76.654
0	-6.80E-02	56.45
5	1.42E+01	17.928
10	1.06E+01	10.544
15	7.81E+00	7.43

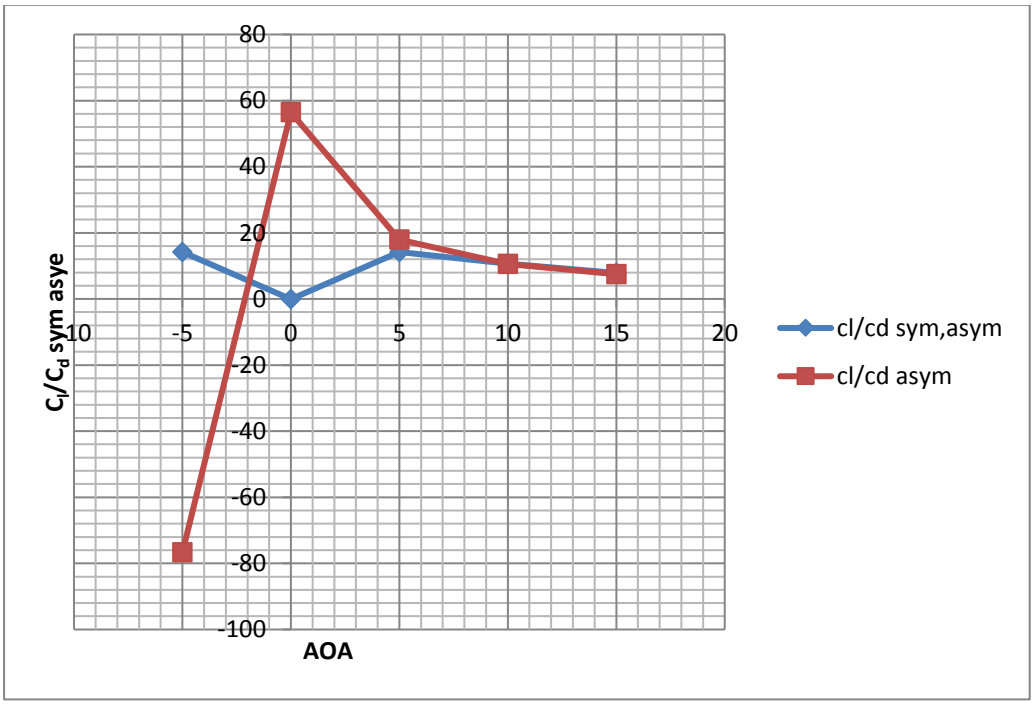

Fig 5.16 C_l / C_d vs. AOA at Mach number 0.4

The graphical representation of the tabulated data of table 5.8 is shown in fig 5.16, The above figure represents C_l / C_d vs. AOA at Mach number 0.4 which shows comparison between symmetric and asymmetric aerofoil where lift to drag ratio is taken on y axis and angle of attack is taken on x axis. Lift to drag ratio represents performance of aerofoil, hence above graph shows performance of asymmetric aerofoil is better than performance of symmetric aerofoil at zero AOA, vice versa at negative AOA and almost similar at positive AOA.

5.3.9 C_l VS Mach number at various angles of attack for Symmetric Aerofoil

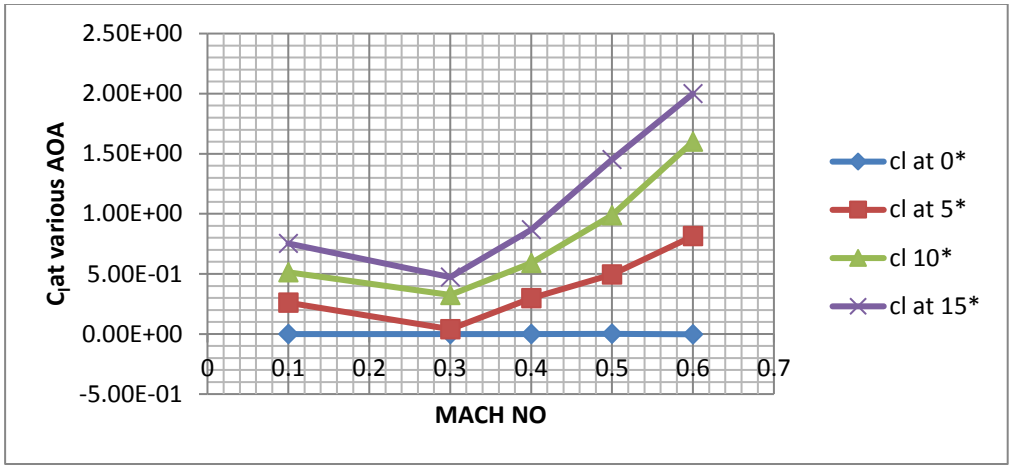

Fig 5.17 C_l vs. Mach no at various AOA at symmetric aerofoil

The above fig 5.17 shows **C_l** vs. Mach number at various AOA for symmetric aerofoil where coefficient of lift is taken on y axis and Mach number is taken on x axis. It shows how coefficient of lift changes for subsonic flow i.e., it decreases up to 0.3 Mach number and then rapidly increases.

5.3.10 C_l VS Mach no at various angles of attack for Asymmetric Aerofoil

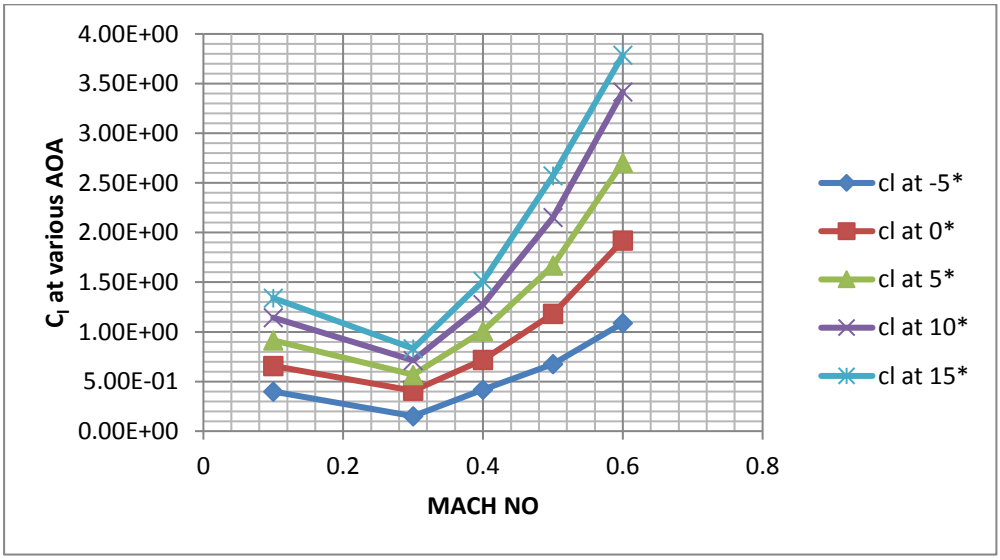

Fig 5.18 C_l vs. Mach no at various AOA of asymmetric aerofoil

The above fig 5.18 shows **C_l** vs. Mach number at various AOA for Asymmetric aerofoil where coefficient of lift is taken on y axis and Mach number is taken on x axis. It shows same result as symmetric aerofoil but here we get much higher coefficient of lift when compared to symmetric aerofoil and coefficient of lift is not zero at zero angle of attack.

5.3.11 C_d vs. Mach no at various angles of attack for Symmetric Aerofoil

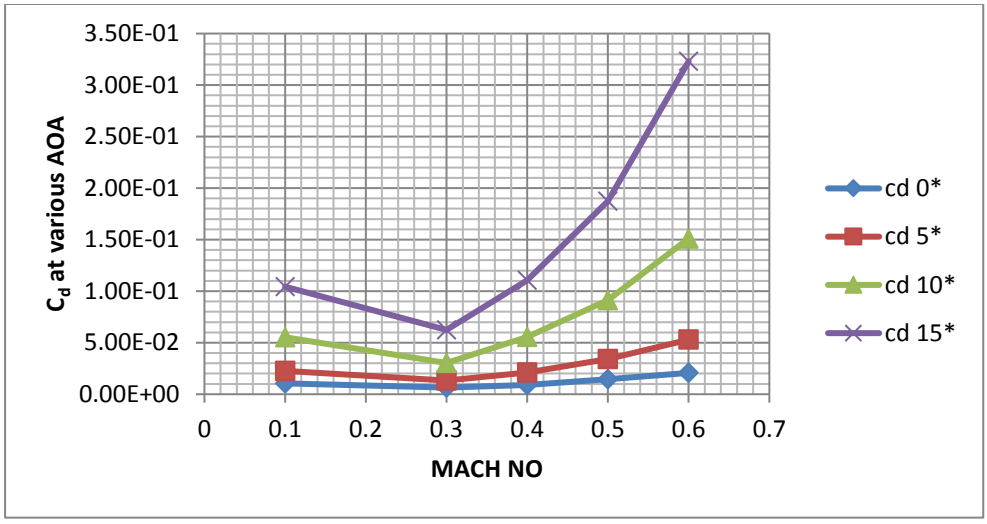

Fig 5.19 C_d vs. Mach no at various AOA of symmetric aerofoil

The above fig 5.19 shows **C_d** vs. Mach number at various AOA for symmetric aerofoil where coefficient of drag is taken on y axis and Mach number is taken on x axis. It shows variation of coefficient of drag with respect to Mach number i.e., as angle of attack increases coefficient of drag also increases.

5.3.12 C_d vs. Mach number at various angles of attack for Asymmetric Aerofoil

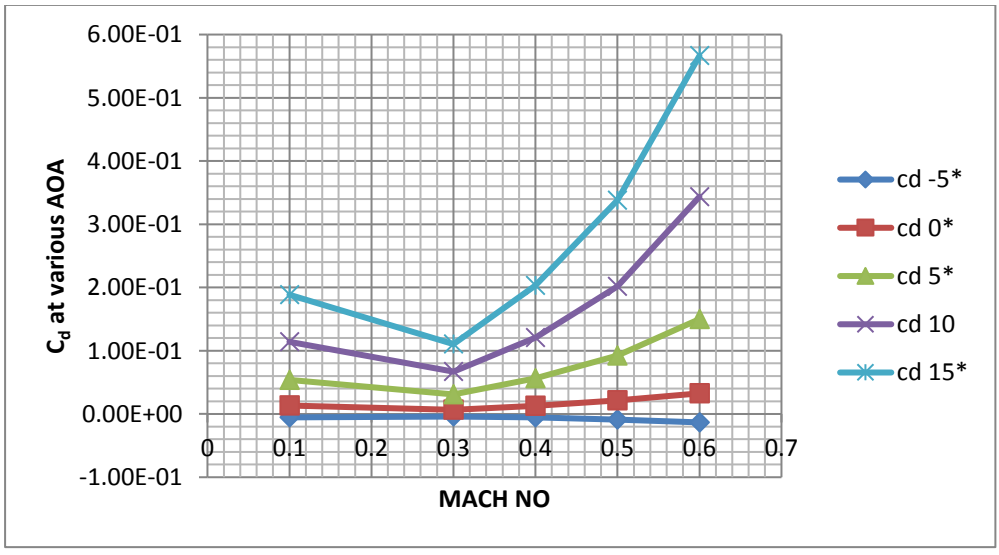

Fig 5.20 C_d vs. Mach no at various AOA of asymmetric aerofoil

The above fig 5.20 shows **C_d** vs. Mach number at various AOA for Asymmetric aerofoil. But here variation in coefficient of drag is higher than symmetric aerofoil.

5.3.13 C_m vs. Mach no at various angles of attack Symmetric Aerofoil

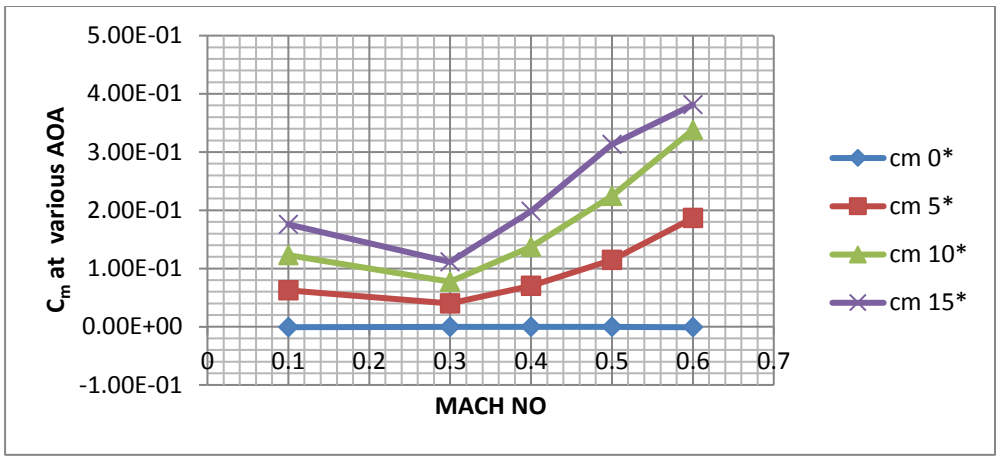

Fig 5.21 C_m vs. Mach no at various AOA of symmetric aerofoil

The above fig 5.21 shows **C_m** vs. Mach number at various AOA for symmetric aerofoil where coefficient of pitching moment is taken on y axis and Mach number is taken on x axis. It shows at zero AOA.

5.3.14 C_m vs. Mach no at various angles of attack Asymmetric Aerofoil

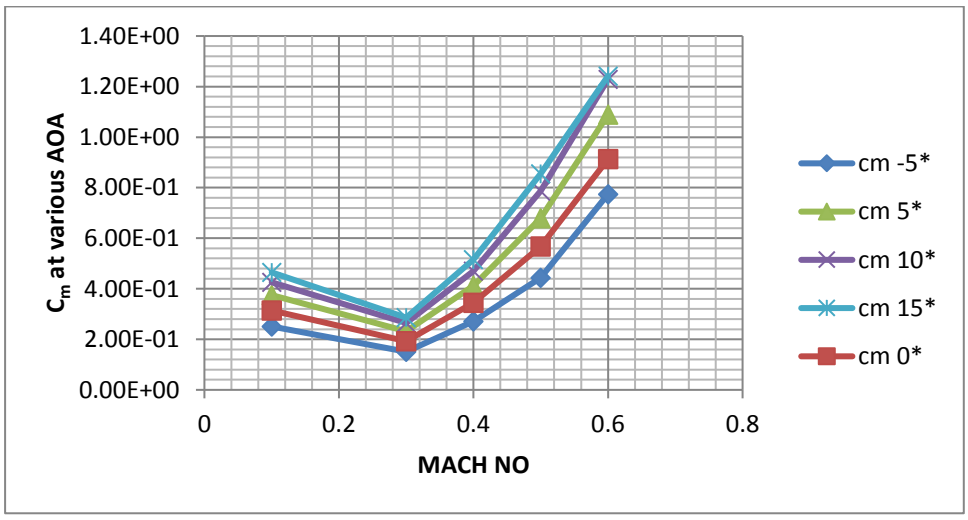

Fig 5.22 C_m vs. Mach no at various AOA of asymmetric aerofoil

The above fig 5.22 shows **C_m** vs. Mach number at various AOA for Asymmetric aerofoil. But here variation in coefficient of pitching moment is lesser than symmetric aerofoil and coefficient of pitching moment is not zero at zero degree AOA as in case of symmetric aerofoil.

6. CONCLUSION

CFD Analysis of NACA 0015 symmetric and NACA 6409 unsymmetrical aerofoils is carried out which has brought a number of valid conclusions as mentioned below. The Conclusions obtained are completely based on analytic results and plots obtained. There are no assumptions or considerations taken to carry out the analysis and the complete work is focused upon comparing the stability and performance of the aerofoil at two different subsonic Mach speeds.

- The Pressure, Velocity & Turbulence Kinetic Energy Contours are found to be appropriate for corresponding Mach inputs and angles of attack.
- The Lift and Drag Coefficients are increasing with increase of angle of attack at taken two different Mach speeds.
- Stall was started with 15° attack angle for NACA 0015, with 16° attack angle for NACA 6409, where lift coefficient decreased and drag coefficient increased.
- The optimum lift coefficient value 1.5 was measured at 16° for NACA 6409 asymmetric aerofoil, for NACA 0015 optimum lift coefficient was measured at 15˚.
- The ratio of Lift to Drag coefficient determines the aerofoil performance which follows the same trend for both the foils.

Finally, lift to drag ratio for NACA 0015 and NACA 6409 aerofoils were compared to find out the better aerofoil. In this case, NACA 6409 asymmetrical aerofoil is better than NACA 0015 symmetrical aerofoil.

7. FUTURESCOPE

Good correlation between wind tunnel data and CFD simulations encourage that future modifications on aerofoil design shall be investigated in simulation software. Though, it is emphasized that wind tunnel experiments must still be done to validate the accuracy of the evolving designs and computer models. Future work on the same subject acquires experimental data for more than one velocity.

REFERENCES

1. Novel Kumar Sahu, Mr. Shadab Imam., "A Review on Transonic Flow over an Aerofoil", International Journal of Innovative Science, Engineering & Technology, Vol. 2, Issue 5, May 2015.

2. Mochammad Agoes Moelyadi., "Improvement of transonic aerofoil Aerodynamic performance with trailing Edge modification using wedge Configuration", ICAS 2002 Congress.

3. Gultop T., "An Investigation of the effect of aspect ratio on Aerofoil performance." Gazi : American Journal of Applied Sciences ISSN/EISSN: 15469239 15543641, Volume: 2, Issue: 2 ,Pages: 545-549 ,1995.

4. Arvind M. "CFD ANALYSIS OF STATIC PRESSURE AND DYNAMIC PRESSURE FOR NACA 4412" International Journal of Engineering Trends and Technology ISSN/EISSN: 22315381 Volume: 4 Issue: 8 Pages: 3258-3265,(2010) .

5. P.Sethunathan, M.Niventhran, V.Siva & R.Sadhan Kumar., "Analysis of Aerodynamic Characteristics of a Supercritical Aerofoil for Low Speed Aircraft", International Journal of Research in Engineering and Technology, eISSN: 2319-1163, pISSN: 2321-7308.

6. Goel S.,(2008) " Turbine Aerofoil Optimization Using Quasi-3D Analysis Codes." International Journal of Aerospace Engineering ISSN/EISSN: 16875974 16875974 Volume: 2009, 2008.

7. Kevadiya M. (2013) CFD "Analysis of Pressure Coefficient for NACA 4412" International Journal of Engineering Trends and Technology ISSN/EISSN: 22315381 Volume: 4 Issue: 5 Pages: 2041-2043, 2013 .

8. Charles H. Carlson, "Preliminary Scramjet Design for Hypersonic Air breathing.Missile Application, NASA Contractor Report 3742, November 1983.

9. N. Ahmed, B.S. Yilbas*, M.O. Budair;" Computational study into the flow field developed around a cascade of NACA 0012 aerofoils". Comput. Methods Appl. Mech. Engrg. 167 (1998) 17-32.

10. D.Rana, S.Patel, AK.Onkar and M.Manjuprasad, "Time domain simulation of aerofoil flutter using fluid structure coupling through FEM based CFD solver", Symposium of Applied Aerodynamics and Design of Aerospace vehicle, SAROD20111, Nov 16-18 2009, Bangalore.

WEBSITE REFERENCES

1. http://www.aerofoiltools.com
2. http://ethesis.nitrkl.ac.in
3. https://www.ijser.org
4. https://en.wikipedia.org/wiki/Airfoil